

การประยุกต์ใช้การกลั่นแบบมีปฏิริยาสำหรับการผลิตเทอร์เชียรี เอมีล เอทิลอีเทอร์

จากเอทานอลและเทอร์เชียรี เอมีล แอลกอฮอล์



นางสาวอรกนก บุญธรรมศิริวุฒิ

สถาบันวิทยบริการ

จุฬาลงกรณ์มหาวิทยาลัย

วิทยานิพนธ์นี้เป็นส่วนหนึ่งของการศึกษาตามหลักสูตรปริญญาวิศวกรรมศาสตรมหาบัณฑิต

สาขาวิชาวิศวกรรมเคมี ภาควิชาวิศวกรรมเคมี

คณะวิศวกรรมศาสตร์ จุฬาลงกรณ์มหาวิทยาลัย

ปีการศึกษา 2548

ISBN 974-53-2749-2

ลิขสิทธิ์ของจุฬาลงกรณ์มหาวิทยาลัย

APPLICATION OF REACTIVE DISTILLATION FOR PRODUCTION OF
TERTIARY AMYL ETHYL ETHER FROM ETHANOL AND TERTIARY AMYL
ALCOHOL



Miss Onkanok Boonthamtirawuti

สถาบันวิทยบริการ
จุฬาลงกรณ์มหาวิทยาลัย

A Thesis Submitted in Partial Fulfillment of the Requirements
for the Degree of Master of Engineering Program in Chemical Engineering

Department of Chemical Engineering

Faculty of Engineering

Chulalongkorn University

Academic Year 2005

ISBN 974-53-2749-2

Thesis Title APPLICATION OF REACTIVE DISTILLATION FOR
 PRODUCTION OF TERTIARY AMYL ETHYL ETHER
 FROM ETHANOL AND TERTIARY AMYL ALCOHOL

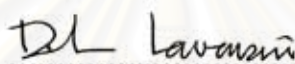
By Miss Onkanok Boonthamtirawuti

Field of Study Chemical Engineering

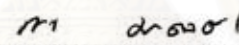
Thesis Advisor Associate Professor Suttichai Assabumrungrat, Ph.D.

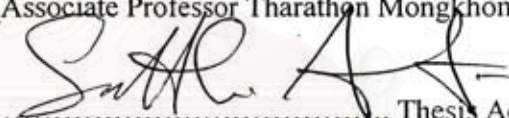
Thesis Co-advisor Amornchai Arpornwichanop, D.Eng.

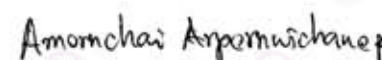
Accepted by the Faculty of Engineering, Chulalongkorn University in Partial
Fulfillment of the Requirements for the Master's Degree

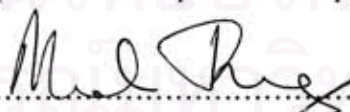

..... Dean of the Faculty of Engineering
(Professor Direk Lavansiri, Ph.D.)

THESIS COMMITTEE


..... Chairman
(Associate Professor Tharathon Mongkhonsi, Ph.D.)


..... Thesis Advisor
(Associate Professor Suttichai Assabumrungrat, Ph.D.)


..... Thesis Co-advisor
(Amornchai Arpornwichanop, D.Eng.)


..... Member
(Assistant Professor Muenduen Phisalaphong, Ph.D.)


..... Member
(Assistant Professor Bunjerd Jongsomjit, Ph.D.)

อรกนก บุญธรรมศิริวุฒิ: การประยุกต์ใช้การกลั่นแบบมีปฏิกิริยาสำหรับการผลิตเทอร์เชียรีเอมีล เอทิลอีเทอร์จากเอทานอลและเทอร์เชียรีเอมีลแอลกอฮอล์ (APPLICATION OF REACTIVE DISTILLATION FOR PRODUCTION OF TERTIARY AMYL ETHYL ETHER FROM ETHANOL AND TERTIARY AMYL ALCOHOL)

อ. ที่ปรึกษา: รองศาสตราจารย์ ดร. สุทธิชัย อัสสะปารุงรัตน์,

อ. ที่ปรึกษาฯร่วม: ดร. อมรชัย อภรณ์วิชานพ, 113 หน้า ISBN 974-53-2749-2

งานวิจัยนี้เกี่ยวข้องกับการคัดเลือกตัวเร่งปฏิกิริยาที่เหมาะสมสำหรับสังเคราะห์สารเทอร์เชียรี เอมีล เอทิล อีเทอร์ (TAE) ซึ่งเป็นสารประกอบออกซิเจนที่สามารถนำมาใช้ทดแทนสารเมทิล เทอร์เชียรี บิวทิล อีเทอร์ (MTBE) จากปฏิกิริยาในวัฏภาคของเหลวระหว่างเทอร์เชียรี เอมีล แอลกอฮอล์ (TAA) และเอทานอล (ETOH) ตัวเร่งปฏิกิริยาที่สนใจ ได้แก่ แอมเบอร์ลิส 15 แอมเบอร์ลิส 16 แอมเบอร์ลิส 36 แอมเบอร์ลิส 131 โดแน็กซ์ 50WX8 ซีโอไลต์ที่มีอัตราส่วนซิลิกอนต่ออะลูมินาเท่ากับ 13.5 และ 40 โดยนำมาทดสอบปฏิกิริยาในเครื่องปฏิกรณ์แบบกึ่งกะที่อุณหภูมิ 353 เคลวิน และความดัน 810.4 กิโลปาสกาล จากการศึกษาพบว่าปฏิกิริยาไฮเดรชันของ TAA เป็นปฏิกิริยาข้างเคียงหลักที่เกิดขึ้นเมื่อพิจารณาจากค่าการเกิดและค่าผลได้พบว่าแอมเบอร์ลิส 16 เป็นตัวเร่งปฏิกิริยาการสังเคราะห์ TAE ได้ดีที่สุดในนั้นจึงนำตัวเร่งปฏิกิริยาแอมเบอร์ลิส 16 มาใช้ในการศึกษาจลนพลศาสตร์ของปฏิกิริยาอีเทอร์ฟิเคชันของ TAA ซึ่งดำเนินการทดลองในเครื่องปฏิกรณ์เดิม ที่อุณหภูมิ 333 343 และ 353 เคลวิน เพื่อใช้ในการคำนวณค่าตัวแปรทางจลนพลศาสตร์ที่แสดงด้วยสมการของ Arrhenius และ Van't Hoff โดยใช้แบบจำลองทางจลนศาสตร์ 2 แบบคือ แบบจำลองของ Langmuir-Hinshelwood (L-H) และ Power Law (PL) ในรูปแบบของค่าความว่างในการอธิบายสมการแสดงอัตราการเกิดปฏิกิริยา จากผลการศึกษาพบว่าแบบจำลอง L-H สามารถอธิบายอัตราการเกิดปฏิกิริยาได้ดีที่สุด นอกจากนี้ในงานวิจัยนี้ยังได้เสนอแบบจำลอง PL ในรูปแบบของค่าสัดส่วนโดยโมล ที่ใช้อธิบายสมการแสดงอัตราการเกิดปฏิกิริยาการสังเคราะห์ TAE ด้วย ทั้งนี้เพื่อนำไปใช้ในโปรแกรม Apen Plus สำหรับการจำลองการกลั่นแบบมีปฏิกิริยา ซึ่งเป็นกระบวนการที่เหมาะสมสำหรับปฏิกิริยาที่ถูกจำกัดด้วยสมดุล โดยในงานวิจัยนี้ได้ทำการศึกษามูลของตัวแปรในการดำเนินการต่างๆ ที่มีต่อสมรรถนะของหอกลั่นแบบมีปฏิกิริยา อันได้แก่ อัตราการป้อนกลับ น้ำหนักของตัวเร่งปฏิกิริยา ตำแหน่งของชั้นสารป้อนและส่วนของชั้นปฏิกิริยา พลังงานความร้อนที่ให้กับหม้อต้มซ้ำ และความดัน

สถาบันวิทยบริการ จุฬาลงกรณ์มหาวิทยาลัย

ภาควิชา.....วิศวกรรมเคมี
สาขาวิชา.....วิศวกรรมเคมี
ปีการศึกษา..... 2548

ลายมือชื่อนิสิต.....
ลายมือชื่ออาจารย์ปรึกษา.....
ลายมือชื่ออาจารย์ที่ปรึกษาฯร่วม.....

4670595221 : MAJOR CHEMICAL ENGINEERING
 KEY WORD : *tert*-AMYL ETHYL ETHER/ REACTIVE DISTILLATION/ ASPEN
 PLUS/ OXYGENATE/ *tert*-AMYL ALCOHOL

ONKANOK BOONTHAMTIRAWUTI : APPLICATION OF REACTIVE
 DISTILLATION FOR PRODUCTION OF TERTIARY AMYL ETHYL
 ETHER FROM ETHANOL AND TERTIARY AMYL ALCOHOL.

THESIS ADVISOR: ASSOC. PROF. SUTTICHAJ ASSABUMRUNGRAT,
 Ph.D., THESIS COADVISOR: AMORNCHAI ARPORNWICHANOP, D.Eng.,
 113 pp. ISBN 974-53-2749-2

This thesis concerns catalyst screening for the synthesis of *tert*-amyl ethyl ether (TAAE), an alternative oxygenate for MTBE replacement, from a liquid-phase reaction between *tert*-amyl alcohol (TAA) and ethanol (EtOH). Various commercial catalysts; i.e., Amberlyst-15, Amberlyst-16, Amberlyst-36, Amberlyst-131, beta-Zeolite with Si/Al = 13.5 and 40, and Dowex 50WX8, were tested by performing the reaction in a semi batch reactor operated at temperature at 353 K and pressure of 810.4 kPa. The dehydration of TAA to IA was found to be a major side reaction in this system. Amberlyst-16 shows the best performance in terms of selectivity and yield. Therefore, it was further investigated in the kinetic study using the same reactor. Three temperature levels of 333, 343 and 353 K were performed to obtain the parameters in the Arrhenius's equation and the Van't Hoff equation. Two activity-based kinetic models of Langmuir-Hinshelwood (L-H) and Power Law (PL) were fitted with the experiment result. It was observed that L-H showed the best reaction rate description. In addition, the mole fraction-based PL model is also included in this study to follow the requirement of the ASPEN PLUS program, which is used in the simulation studies of reactive distillation, a promising process for equilibrium-limited reactions. The effects of various operating parameters such as reflux ratio, catalyst weight, location of feed stage and reaction section, heat duty and operating pressure on the reactive distillation performance were simulated.

สถาบันวิทยบริการ
 จุฬาลงกรณ์มหาวิทยาลัย

DepartmentChemical Engineering.....

Field of Study .Chemical Engineering.....

Academic year2005.....

Student's signature

Advisor's signature

Co-advisor's signature

Onkanok B.

Suttichai

Amornchai Arpornwichanop

ACKNOWLEDGEMENTS

The author wishes to express her sincere gratitude and appreciation to her advisor, Associate Professor Suttichai Assabumrungrat, and coadvisor, Dr. Amornchai Arpornwichanop for their valuable suggestions, stimulating, useful discussions throughout this research and devotion to revise this thesis; otherwise, this research work could not be completed in a short time. In addition, the author would also be grateful to Associate Professor Tharathon Mongkhonsi, as the chairman, Assistant Professor Bunjerd Jongsomjit, and Assistant Professor Muenduen Phisalaphong as the members of the thesis committee. The supports from National Research Council of Thailand, TJTTP-JBIC, and Graduate school of Chulalongkorn University are also gratefully acknowledged.

Most of all, the author would like to express her highest gratitude to her parents who always pay attention to her all the times for suggestions and their wills. The most success of graduation is devoted to her parents.

Finally, the author wishes to thank the members of the Center of Excellence on Catalysis and Catalytic Reaction Engineering, Department of Chemical Engineering, Faculty of Engineering, Chulalongkorn University for their assistance.

สถาบันวิทยบริการ
จุฬาลงกรณ์มหาวิทยาลัย

TABLE OF CONTENTS

	PAGE
ABSTRACT (IN THAI)	iv
ABSTRACT (IN ENGLISH)	v
ACKNOWLEDGEMENTS	vi
TABLE OF CONTENTS	vii
LIST OF TABLES	xi
LIST OF FIGURES	xiii
NOMENCLATURE	xvi
CHAPTER	
I INTRODUCTION	1
II THEORY	5
2.1 Oxygenate Compound.....	5
2.2 TAE.....	8
2.3 Ion Exchange Resin.....	9
2.3.1 Physical Structure of Resin.....	9
2.3.2 Chemical Structure of Resin.....	11
2.3.3 Physical and Chemical Properties of Ion Exchange Resins.....	12
2.3.3.1 Crosslinkage.....	12
2.3.3.2 Particle Size	14
2.3.3.3 Pressure Drop.....	15
2.4 Zeolite.....	16
2.4.1 Structure of Zeolite.....	16
2.4.2 Properties of Zeolite.....	17
2.4.3 Solid Heterogeneous Catalyst: Beta Zeolite....	18

	PAGE
2.5	Reactive Distillation..... 20
2.5.1	Reactive Distillation Configurations..... 20
2.5.2	Advantages of Reactive Distillation..... 22
2.6	Aspen Plus..... 23
2.6.1	Features of Aspen Plus..... 23
2.6.2	Benefits of Aspen Plus..... 24
III	LITERATURE REVIEWS..... 25
3.1	Production of Tertiary-Amyl Ethyl Ether..... 25
3.1.1	Production of TAEE from IA and EtOH..... 26
3.1.2	Production of TAEE from TAA and EtOH..... 29
3.2	Application of Reactive Distillation for Octane Enhancing Ether Production..... 31
IV	EXPERIMENT..... 34
4.1	Catalyst Screening 34
4.1.1	Semi Batch Reactor Apparatus..... 34
4.1.2	Chemical Materials..... 35
4.1.3	Catalysts..... 36
4.1.4	Experimental Procedure..... 37
4.1.5	Analysis..... 37
4.2	Kinetics Study..... 38
4.2.1	Experimental Procedure of TAA Dehydration.... 39
4.2.2	Experimental Procedure of TAA Etherification.. 39
4.2.3	Analysis..... 39

	PAGE
4.3	Reactive Distillation Study..... 39
4.3.1	Reactive Distillation Apparatus..... 40
4.3.2.	Experiment Procedure of Reactive Distillation ... 43
4.3.2.1.	Reactive Distillation Experiment in Laboratory..... 43
4.3.2.2.	Reactive Distillation Simulation by Aspen Plus Program..... 43
4.3.3.	Analysis..... 44
V	RESULTS AND DISCUSSION..... 45
5.1	Catalyst Screening..... 45
5.2	Kinetic Study..... 47
5.2.1	Development of Mathematical Models..... 47
5.2.2	Kinetic Parameter Determination..... 50
5.2.2.1	TAA Dehydration..... 50
5.2.2.2	TAA Etherification..... 55
5.3	Reactive Distillation Study..... 60
5.3.1	The Performance of Reactive Distillation at Standard Condition..... 61
5.3.2	Effect of Operating Parameters..... 63
5.3.2.1	Effect of Reflux Ratio..... 64
5.3.2.2	Effect of Location of Feed Stage and Reaction Section..... 65
5.3.2.3	Effect of Catalyst Weight..... 67
5.3.2.4	Effect of Heat Duty..... 68
5.3.2.5	Effect of Operating Pressure..... 69

	PAGE
VI CONCLUSIONS AND RECOMMENDATIONS.....	71
6.1 Conclusions.....	71
6.1.1 Catalyst Screening.....	71
6.1.2 Kinetic Study.....	72
6.1.3 Reactive Distillation Study.....	73
6.2 Recommendations.....	74
REFERENCES	75
APPENDICES	
APPENDIX A PRETREATMENT PROCEDURE OF BETA ZEOLITE WITH Si/Al RATIO OF 13.5.....	80
APPENDIX B CALIBRATION CURVE.....	81
APPENDIX C UNIFAC METHOD.....	83
APPENDIX D MODIFIED KINETIC PARAMETERS OF TAE SYNTHESIS FOR APPLICATION IN ASPEN PLUS PROGRAM.....	91
VITA	95

LIST OF TABLES

TABLE	PAGE
2.1 Physical properties of oxygenated compounds.....	7
2.2 Physical, chemical and thermal properties of TAEE	8
2.3 Diameter of particles related to mesh range	14
4.1 Details of chemicals use in the study	35
4.2 Various commercial catalysts.....	36
4.3 Operating conditions of gas chromatography	38
4.4 Standard operating conditions of reactive distillation	40
5.1 Summary of performance for various catalysts at 12 th hours...	47
5.2 RMSD value of kinetic model in each temperature of TAA dehydration reaction.....	51
5.3 Kinetic constant and activation energy of TAA dehydration...	53
5.4 RMSD value of kinetic model in each temperature of TAA etherification reaction.....	55
5.5 Reaction rate constants and values of activation energy	58
5.6 Sorption equilibrium constant and values of the adsorption enthalpies and adsorption entropies of H ₂ O and EtOH.....	59
5.7 Comparison the value of activation energy with other researches..	60
5.8 Adsorption entropies of H ₂ O and EtOH and value from literature.....	60
5.9 Comparison of experimental and simulation results.....	61
5.10 Effect of location of feed stage and reaction section on conversion of TAA and selectivity of TAEE and composition in bottom.....	66
C.1 UNIFAC-VLE subgroup parameters.....	88
C.2 UNIFAC-VLE group interaction parameter a_{mk} , in Kelvins..	89

TABLE	PAGE
C.3 UNIFAC-VLE subgroup parameters (for TAEE synthesis system).....	90
C.4 UNIFAC-VLE interaction parameters, a_{mk} , in Kelvins (for TAEE synthesis system).....	90
D.1 The values of kinetic constant and activation energy in activity-based PL model.....	91
D.2 Average activity coefficient calculated by MATLAB.....	92
D.3 Modified kinetic constant and activation energy for this study...	94



สถาบันวิทยบริการ
จุฬาลงกรณ์มหาวิทยาลัย

LIST OF FIGURES

FIGURE	PAGE
2.1 Molecular structure of TAEE.....	8
2.2 Ion exchange resin beads.....	9
2.3 Structure of beta zeolite	19
2.4 Conventional process involving reaction followed by separation	21
2.5 Application of reactive distillation for low volatility product process.....	21
4.1 Schematic diagram of the catalyst selection experimental set-up.....	35
4.2 Schematic diagram of reactive distillation system.....	41
4.3 Schematic diagram of RADFRAC reactive distillation column	42
5.1 Performances of various catalysts: (a) conversion of TAA, (b) yield of TAEE.....	46
5.2 Mole profile of TAA dehydration reaction component (P = 810.4 kPa, $m_r = 2$ g, $n_{TAA} = 0.6$ mole, $n_{EtOH} = 0.6$ mole): (a) at 333 K, (b) at 343 K, (c) at 353 K (symbols: experiment results, solid lines: L-H.A model, dashed lines: PL.A model).....	52
5.3 Arrhenius's plot of TAA dehydration	53
5.4 Sorption equilibrium constant of H ₂ O at different temperature.....	54
5.5 Mole profile of TAA etherification reaction component (810.4 kPa, $m_r = 2$ g, $n_{TAA} = 0.6$ mole, $n_{EtOH} = 0.6$ mole): (a) at 333 K, (b) at 343 K, (c) at 353 K (symbols: experiment results, solid lines: L-H.A model, dashed lines: PL.A model, and dash dot lines: PL.X model).....	56
5.6 Arrhenius' s plots (symbols: ● = k_1 , Δ = k_2 , ■ = k_3 , dashed lines: PL.A model, solid lines: L-H.A model, and dash dot lines: PL.X model)..	57

FIGURE	PAGE
5.7 Van't Hoff plots for sorption equilibrium constant of H ₂ O and EtOH.....	58
5.8 Mole fraction profiles and temperature of distillate at standard operating condition (weight of catalyst to feed flow rate ratio = 3.2 kg/(mol/min), reflux ratio = 10, and molar ratio of TAA:EtOH = 1:1).....	62
5.9 Mole fraction profiles and temperature of bottom at standard operating condition (weight of catalyst to feed flow rate ratio = 3.2 kg/(mol/min), reflux ratio = 10, and molar ratio of TAA:EtOH = 1:1).....	62
5.10 Mole fraction and temperature profiles at standard condition change with stages (weight of catalyst to feed flow rate ratio = 3.2 kg/(mol/min), reflux ratio = 10, and molar ratio of TAA:EtOH =1:1).....	63
5.11 Effect of reflux ratio on conversion of TAA, selectivity and yield of TAEE (catalyst = Amberlyst 16, catalyst weight to feed flow rate = 3.2 kg/(mole/min), heat duty = 67.5 W, pressure = 101.3 kPa and molar ratio of TAA: EtOH = 1:1).....	64
5.12 Effect of catalyst weight on conversion of TAA, selectivity and yield of TAEE (catalyst = Amberlyst 16, heat duty = 67.5 W, pressure = 101.3 kPa and molar ratio of TAA:EtOH = 1:1).....	67
5.13 Effect of Heat duty on conversion of TAA and selectivity of TAEE (catalyst = Amberlyst 16, catalyst weight to feed flow rate = 3.2 kg/(mole/min), heat duty = 67.5 W, pressure = 101.3 kPa and molar ratio of TAA: EtOH = 1:1).....	68
5.12 Effect of operating pressure on conversion of TAA , selectivity and yield of TAEE (catalyst = Amberlyst 16, catalyst weight to feed flow rate = 3.2 kg/(mole/min), reflux ratio = 10, heat duty = 67.5 atm and molar ratio of TAA: EtOH = 1:1).....	70

FIGURE	PAGE
5.15 Effect of operating pressure on temperature of each stage (catalyst = Amberlyst 16, catalyst weight to feed flow rate = 3.2 kg/(mole/min), reflux ratio = 10, heat duty = 67.5 atm and molar ratio of TAA: EtOH = 1:1).....	70
B.1 Chromatograms of all components in TAEE synthesis system (integration parameters: width = 5 sec, stop time = 35 min, speed = 2 mm/min, slope = 30 uV/min, atten = 5 mV, min. area = 100 count).....	81
B.2 Calibration curves of all components in TAEE synthesis system (a) TAA, (b) EtOH, (c) IA, (d) H ₂ O and (e) TAEE.....	82
D.1 Arrhenius's plot of $k_{l,x}$	94

NOMENCLATURE

a_i	activity of species i	[-]
E_a	activation energy	[J/mol]
$\Delta_r G$	Gib's free energy of the reaction	[kJ/s]
ΔH_r	standard enthalpy change of the reaction	[kJ/s]
$k_{j,a}$	kinetic constant based on activity	[mol/(s mol-H ⁺)]
$k_{j,x}$	kinetic constant based on mol fraction	[mol/(s mol-H ⁺)]
$K_{eq,j}$	chemical equilibrium constant	[-]
K_i	sortion equilibrium constant	[-]
LD	liquid distillate flow rate	[mol/s]
L	liquid flow rate returning from stage 1 to stage 2	[mol/s]
m_r	mass of dry ion-exchange resin	[kg]
M	number of components	[-]
M_i	molecular weight of species i	[kg/mol]
n_i	number of mole of species i in the reactor	[mol]
Q_r	ion-exchange capacity (= 5.0)	[meq-H ⁺ /kg-dry resin]
Q	reboiler duty	[W]
r_j	reaction rate	[mole/(s meq -H ⁺)]
R	residue flow rate	[mol/s]
R_g	gas constant (=8.314)	[J/(mol/K)]
$\Delta_r S$	standard entropy change of the reaction	[J/(mol/K)]
T	operating temperature	[K]
x_i	mole fraction of component i	[-]
$RMSD_i$	Relative Root Mean Square Deviation	[-]
X_{TAA}	conversion of TAA	[-]
S_{TAEE}	selectivity of TAEE	[-]
Y_{TAEE}	yield of TAEE	[-]

Greeks letters

γ_i activity coefficients of species i [-]

Subscripts

i species i
 j order of reaction
 a activity
 x mole fraction
 Exp experimental result
 Sim simulation result

Abbreviations

CO carbon monoxide
 CSTR continuous stirred tank reactor
 DME dimethyl ether
 DEE diethyl ether
 ETBE ethyl tertiary butyl ether
 EtOH ethyl alcohol
 H₂O water
 IA isoamylene
 KHSO₄ potassium hydrogen sulfate
 L-H Langmuir-Hinshelwood
 LH.A activity based Langmuir-Hinshelwood
 LH.X mole fraction based Langmuir-Hinshelwood
 MeOH methanol
 MTBE methyl tertiary butyl ether
 NO_x oxides of nitrogen
 PFR plug flow reactor
 PL Power Law
 PL.A activity based Power Law
 PL.X mole fraction based Power Law
 TAA tert-amyl alcohol

TAEE tert-amyl ethyl ether
TAME tert-amyl methyl ether



สถาบันวิทยบริการ
จุฬาลงกรณ์มหาวิทยาลัย

CHAPTER I

INTRODUCTION

Over the past years, the global environment has been impacted from combustion emission and conventional gasoline's evaporation. An oxygenated compound is a key component to be added to gasoline for pollution reduction and improvement of combustion efficiency, thereby reducing carbon monoxide, CO content and hydrocarbon emission from exhaust pipe. Therefore, the use of oxygenated compounds has increased rapidly. Nevertheless, it has been known that oxygenated compounds can generally increase the emission of oxides of nitrogen (NO_x) which are the significant cause of acid rain and photochemical smog. For this reason, the oxygen content in the gasoline for automobile engines is limited to control NO_x emission.

Oxygenate compounds can be divided into two groups: alcohols, e.g. methanol (MeOH), ethanol (EtOH), and tertiary amyl alcohol (TAA) and ethers, e.g. methyl tertiary butyl ether (MTBE), ethyl tertiary butyl ether (ETBE) and higher tertiary ethers. Although MTBE has been widely used in many countries, it can contaminate the underground water because of its high water solubility. Furthermore, it was found to be hardly degraded in both of aerobic (Stefan et al. 1997; Mo et al. 1997; Salanitro et al., 1994) and anaerobic condition (Yeh and Novak, 1994). Therefore, other oxygenated compounds such as ETBE, higher tertiary ethers, e.g. 2-methoxy-2-methylbutane (tert-amyl methyl ether, TAME) and 2-ethoxy-2-methylbutane (tert-amyl ethyl ether, TAEE) have been of interest nowadays. Even though, researches of ETBE have rapidly increased in recent years, its structure seems to be quite similar to MTBE, and should encounter the same problems soon. Higher tertiary ethers such as TAME and TAEE have been attractive because they have lower water solubility and lower blending Reid vapor Pressure (bRvp) than MTBE. The low bRvp of TAME (1.5 psi) and TAEE (1.2 psi) as less bRVP than 7.8 psi (Cunill et.al, 1993) are required for some hot places during summer or some topical countries, like Thailand.

TAAE seems to be more interesting than TAME as ethanol, one of the reagents for TAAE synthesis, can be produced from renewable sources such as sugar, corn and molasses. The other reagent for TAAE synthesis can be either tertiary amyl alcohol (TAA) or isoamylene (IA). However, most of previous works have been focused on the use of IA which is found mainly in the C₅ fraction of FCC gasoline and in the product streams of an ethane cracker including a product from dehydrogenation of isopentane. TAA is an alternative reagent instead of IA. It can directly react with ethanol, or indirectly dehydrated to IA and then react with ethanol. Furthermore, TAA is a major product of fusel oil from biomass fermentation process (Aiouche and Goto, 2003a); therefore, the synthesis of TAAE from TAA and ethanol is derived from renewable sources absolutely.

Conventionally, ether synthesis is carried out in liquid phase system catalyzed by many strong acid catalysts; i.e. homogeneous catalysts such as sulfuric acid and heterogeneous catalysts such as strong acidic ion exchange resin and acidic zeolite. However, the homogeneous catalysts are sensitive to the present of water in a feed solution and the desired product is difficult to be separated from a product solution. Therefore, the heterogeneous catalysts are a favorable choice. There are a number of works considering the TAAE synthesis using various acidic heterogeneous catalysts, e.g. Amberlyst 16 (Rihko and Krause, 1993; Rihko et al., 1994, 1997, 1998; Linnekoski et al., 1999; Palakkoinen et al., 1998), Amberlyst 15 (Kitchaiya and Datta, 1995; Aiouache and Goto, 2003a, 2003b; Sahapatsombud et al., 2005), and Dowex M32 (Rihko and Krause, 1993).

Reactive distillation (RD), a multifunctional process which combines two conventional processes of reaction and separation, has received much attention. It is suitable for many reactions particularly those limited by chemical equilibrium. The most important benefit of reactive distillation is a reduction in capital investment and energy consumption. Reactive distillation was first used by the chemical and petrochemical industry in esterification processes such as methyl acetate synthesis, ethyl acetate synthesis (Bessling et al., 1998; Okur and Bayramoglu, 2001) to separate reaction products from reactants and to increase product yields (Venkataraman et al., 1990). In 1980s, reactive distillation was carried out for the processes of etherification; MTBE synthesis (Thiel et al., 1997; Eldarsi and Douglas, 1998;

Collignon et al., 1999; Baur et al., 2000), ETBE synthesis (Matouq et al., 1996; Tian and Tade, 2000) and TAME synthesis (Mohl et al., 1997; Thiel et al., 1997). Recently, the study of a hybrid process of reactive distillation and pervaporation membrane reactor (PVR) was performed to reach higher chemical conversion and selectivity in direct TAAE synthesis by Aiouche and Goto (2003b). Presently, reactive distillation has been widespread and achieved for several applications of chemical processes beyond the esterification and etherification; for example, hydrogenation, hydrodesulphurization and isomerization.

Apart from experimental studies, there are many studies focusing on simulation of reactive distillation in order to investigate the effect of operating conditions and design parameters on the performance of reactive distillation. A number of works on the simulation of ether synthesis have been published. Young and Lee (2003) studied the simulation of synthesis ETBE in reactive distillation to design the optimal process. Moreover, Quitian et al. (1999b) proposed a process for industrial production of ETBE by using ASPEN PLUS program. Another simulation of reactive distillation column for ETBE was introduced by Yang et al. (2001). They developed a mathematical model of continuous reactive distillation. For the simulation of TAAE, there are limited numbers of works to study the effect of the operating factors on the column performance. Aiouche and Goto (2001b) studied the synthesis of TAAE from TAA and ethanol in a hybrid column of reactive distillation packed with Amberlyst 15 and pervaporation module. More detailed studies are required to further improve the performance of reactive distillation for the synthesis of TAAE. Then, Sahapatsombud et al. (2005) used Aspen Plus program to simulate TAAE synthesis from TAA and ethanol in reactive distillation by using Amberlyst 15 as catalyst. The effects of various operating parameters were also investigated.

Although TAEЕ seems to be an attractive oxygenated compound for future use, there are still very limited works on the synthesis of TAEЕ using reactive distillation. This research focuses on the application of reactive distillation to produce TAEЕ from TAA and ethanol and the objectives are;

1. To screen the best catalysts for the synthesis of TAEЕ from TAA and EtOH.
2. To study the reaction kinetic for the synthesis of TAEЕ from TAA and EtOH with the selected catalyst.
3. To study the effect of operating conditions on the performance of a reactive distillation for the synthesis of TAEЕ.



สถาบันวิทยบริการ
จุฬาลงกรณ์มหาวิทยาลัย

CHAPTER II

THEORY

This chapter provides some background information necessary for understanding the synthesis of TAAE from TAA and ethanol in reactive distillation by the various acid catalysts. Some detail of oxygenates compound, TAAE, catalysts (ion exchange resin and zeolite), reactive distillation, and Aspen Plus Program are provide in the following section.

2.1 Oxygenated Compound

Oxygenates are compounds containing oxygen in a chain of carbon and hydrocarbon atoms. Their structure provides a reasonable anti-knock value, thus they can be utilized to replace aromatics in gasoline. In addition, the advantage of using the oxygenate agents is to reduce smog-forming tendencies of the exhaust gases. Generally, oxygenates used in gasoline can be classified into two groups; alcohols (C_x-O-H) or ethers (C_x-O-C_y), which contain 1 to 6 carbon atoms. Alcohols have been used in gasoline since the 1930s while MTBE was first used in commercial gasoline in Italy in 1973 and in the US by ARCO in 1979. In 1996, over 95% of gasoline used in California was blended with MTBE. Oxygenate can be derived from fossil fuels such as methanol (MeOH), methyl tertiary butyl ether (MTBE), tertiary amyl methyl ether (TAME), or from biomass such as ethanol (EtOH), ethyl tertiary butyl ether (ETBE) and tert amyl ethyl ether (TAAE). They have significantly different physical properties compared to hydrocarbons as shown in Table 2.1. Oxygenates are beneficial to gasoline function in two ways. Firstly, they have higher blending octane number, so they can replace high octane aromatics in the fuel. These aromatics are responsible for disproportionate amounts of CO and HC exhaust emissions. This is called the “aromatic substitution effect”. Oxygenates can also be used in engines without sophisticated engine management systems to move to the lean side of stoichiometry, thus reducing emission of CO (2% oxygen can reduce CO by 16%) and

HC (2% oxygen can reduce HC by 10%). However, on vehicles with engine management systems, the higher fuel volume is required to bring the stoichiometry back to the preferred optimum setting. Oxygen in the fuel cannot contribute energy and consequently the fuel has less energy content. For the same efficiency and power output, more fuel has to be burnt, and the slight improvements in combustion efficiency that oxygenates provide on some engines usually do not completely compensate for the oxygen.



สถาบันวิทยบริการ
จุฬาลงกรณ์มหาวิทยาลัย

Table 2.1 Physical properties of oxygenated compounds^a

Properties	Ethers				Alcohols			
	MTBE	ETBE	TAME	TAAE	TBA	TAA	MeOH	EtOH
CAS No.	1634-04-4	637-92-3	994-05-08	919-94-8	75-65-0	75-85-4	67-56-1	64-17-5
RON ^b	117	118	112	105	94	NA	133	129
MON ^c	101	101	98	95	100	NA	105	102
Mol. Wt.	88.15	102.18	102.18	116.2	74.12	88.15	32.04	46.07
BP(°C)	55.2	67	86	106	82.2	102	64.6	78.3
Density (g/mL)	0.741	0.752	0.764	0.761	0.786	0.805	0.791	0.795
Water Solubility (mg/l)	43,000 -54,300	26,000	20,000	4,000	Miscible	120	Miscible	Miscible
Blending RVP (psi)	8	4.7	1.5 ^d	1.2 ^d	9	NA	40	18
Neat RVP (psi) 100 °F	7.8	4	2.5	1.2	1.7	NA	NA	2.3
Oxygen(%w)	18.2	15.7	15.7	13.8	21.6	18.15	49.9	34.8

a: Multiple sources; The Handbook of MTBE and Other Gasoline Oxygenates, Mealey's MTBE Conference.

b: RON = Research Octane Number simulates fuel performance under low severity engine operation with engine speed 600 rpm.

c: MON = Motor Octane Number simulates more severe operation that might be incurred at high speed or high load with engine speed 900 rpm.

d: Reid Vapor Pressure, RVP

NA = Not available

2.2 TAEE

Tertiary-amyl ethyl ether (TAEE) is produced by reaction of a branched C₅ olefin called tertiary-amylene with ethanol. TAEE has a higher boiling point, lower octane value than MTBE, and is fully compatible with gasoline hydrocarbon blends. Typical properties of TAEE are listed in Table 2.2 and its molecular structure is given below.

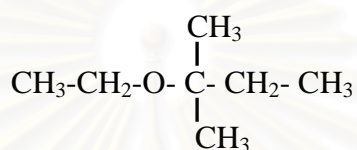


Figure 2.1 Molecular structure of TAEE

Table 2.2 Physical, chemical and thermal properties of TAEE

Molecular formula	C ₇ H ₁₆ O
Molecular weight	116
Elemental analysis	
Carbon content, wt%	72.4
Hydrogen content, wt%	13.8
Oxygen content, wt%	13.8
C/H ratio	4.5
Specific gravity, g/cm ³	0.70
Reid vapor pressure at 25 °C, mmHg	1.2
Boiling point at 760 mmHg, °C	101
Solubility of TAEE in water at 20 °C, wt%	0.4
Blending octane number ^a	
RON	105
MON	95
(RON+MON)/2	100

^a Obtained by adding 10 vol% TAEE to a base gasoline having RON clear = 94.3 and MON clear = 84.3

2.3 Ion Exchange Resin

An ion exchange resin is an insoluble polymeric matrix or support structure, usually supplied as white or yellowish bead (shown in Figure 2.2) and with electrically charged sites at which one ion may replace another in a process called ion exchanging.



Figure 2.2 Ion exchange resin beads.

2.3.1 Physical Structure of Resin

Generally, ion exchange resin can be manufactured from a material which has basic requirements of ion exchange bead. It must be insoluble under normal operating condition, and must be uniform dimension form of sphere. The swelling and contraction of resin bead during exhaustion and regeneration must not cause the bead to burst. In addition, the active site must be permanently attached to the bead. Usually, there are two physical structures of resin; i.e. micro porous and macro porous resin.

Micro porous resin (also called gel resin) is generally a translucent and homogenous crosslink polymer. It does not have permanent pore structure. Therefore, it has no measurable porosity, generally considered to be quite small, usually less than 30 \AA and referred as gellular pore or molecular pores. The pore structure is determined by the distance between the polymer chains and crosslinks which depends on the % crosslinkage of the polymer, the polarity of the solvent, and the operating condition. Normally, it has higher operating efficiencies and lower cost than macro porous resin.

Macro porous resin (also called macroreticular resin) is a large multichannel porous structure and it can be made of two continuous phases; a continuous pore phase and a continuous gel polymeric phase which is structurally composed of small spherical micro gel particles agglomerated together to form cluster, which are fastened together at the interfaces and form inter-connecting pore. It not only has high effective surface area to facilitate ion exchange process and to give access to the exchange site for large ion but also give better physical stability, primarily because of its sponge like structure which gives more stress relief, and better oxidation resistance. Unfortunately, the multi-channel porous structure like sponge allows the active portion of the bead to contain a high level of DVB crosslinking without affecting the exchange kinetics; it means that it has a lower capacity because the beads contain less exchange sites. The “pore” can take up to 10 to 30 % of the polymer which is the reason to reduce the ion exchange capacity proportionately.

Usually, synthetic ion exchange resins are cast as porous beads with considerable external and pore surface where ions can attach. Whenever there is a great surface area, adsorption plays a role. If a substance is adsorbed to an ion exchange resin, no ion is liberated. While there are numerous functional groups that have charge, only a few are commonly used for principle ion exchange resins. These are:

1. Strongly acidic; sulfonic acid groups $-\text{SO}_3\text{H}$ which is strongly ionized to $-\text{SO}_3^-$
2. Strongly basic; $-\text{NR}_3^+$ that has a strong, permanent charge. (R stands for some organic group)
3. Weakly acidic; carboxylic acid groups $-\text{COOH}$ which is weakly ionized to $-\text{COO}^-$
4. Weakly basic; $-\text{NH}_2$ that weakly attracts protons to form NH_3^+ , -secondary and tertiary amines that also attract protons weakly

These groups are sufficient to allow selection of a resin with either weak or strong positive or negative charges.

2.3.2 Chemical Structure of Resin

Commonly, there are two basic types of chemical structures; styrene and acrylic matrix material while divinylbenzene (DVB) is still used as a crosslinker in these matrixes.

The acrylic based material is straight chained hydrocarbons based on polyacrylate and polymethacrylate. The active exchange site of acrylic differing from the styrene is part of the physical structure. The acrylic based material is advantageous in application where organics are presented because it does not foul nearly as much as a styrene based material. However, when an acrylic resin chemically degrades, which is the weak link beyond the physical structure. Furthermore, when an acrylic resin oxidizes, it will swell and become mushy, therefore is usually limited to industrial application. Presently, most ion exchange resins are manufactured by using styrene as the matrix material.

Ion exchange resin based on the copolymerization of styrene and DVB the most commonly used in the world today has been developed since 1944 by an American scientist, D' Alelio and is referred to as being gellular in structure. DVB is the cross linking agent, link together the back bone of styrene polymer contributed to three dimension of the network, fashion it insoluble and determines to what extent the resin is free to swell and shrink. The term "Cross linkage" in a styrene – DVB resin refers to the fraction of DVB. For example, 8 percent crosslinkage means that it contain 92 percent of styrene and 8 of percent DVB. Resins are available today with a DVB content of from 2 to 20% or higher. Higher DVB content gives the bead additional strength but the additional crosslinking can hinder kinetic by making the bead too resistant to the shrinking when in contact with non polar solvent and to swelling when charging from one ionic form to another form, during normal operating.

2.3.3 Physical and Chemical Properties of Ion Exchange Resins

Since ion exchange resin is the copolymer of styrene and DVB, it has most of ideal network properties consisting of a structure resistant to breakage, mechanical wear, oxidation or reduction, uniform of shape in small spheres with good hydraulic properties and insoluble in solvents. However, the properties of resin depend on three main factors; the crosslinkage of styrene and DVB, the particle size of resin, and the pressure drop. These factors are important parameters to describe several properties; that is, moisture content, capacity, equilibration rate, selectivity for various ions, porosity, and flow rate of solution and physical stability.

2.3.3.1. Crosslinkage

The amount of crosslinking depends on the proportions of different monomers used in the polymerization step. Practical ranges are 4 % to 16 %. Resins with very low crosslinking tend to be watery and change dimensions markedly depending on which ions are bound. Properties that are interrelated with crosslinking are:

1. Moisture Content

A physical property of the ion exchange resins that varies with changes in crosslinkage is the moisture content of the resin. For example, sulfonic acid groups attract water, and this water is tenaciously held inside each resin particle. The quaternary ammonium groups of the anion resins behave in a similar manner.

2. Capacity

The total capacity of an ion exchange resin is defined as the total number of chemical equivalents available for exchange per some unit weight or unit volume of resin. The capacity may be expressed in terms of mole-equivalents per unit mass of dry resin or in terms of mole-equivalents per unit volume of wet resin.

Generally, the resins have the higher crosslinked, the more difficult to introduce additional functional groups. Sulfonation is carried out after the crosslinking has been completed and the sulfonic acid groups are introduced inside the resin particle as well as over its surface. Likewise, the quaternary ammonium groups are introduced after the polymerization has been completed and they also are introduced both inside the particle as well as on its surface. Fewer functional groups can be introduced inside the particles when they are highly crosslinked and hence the total capacity on a dry basis drops slightly.

This situation is reversed when a wet volume basis is used to measure the capacity on a resin. Although fewer functional groups are introduced into a highly crosslinked resin, these groups are spaced closer together on a volume basis because the volume of water is reduced by the additional crosslinking. Thus the capacity on a wet volume basis increases as cross-linking increases.

3. Equilibration Rate

Ion exchange reactions are reversible reactions with equilibrium conditions being different for different ions. Crosslinkage has a definite influence on the time required for an ion to reach equilibrium. An ion exchange resin that is highly crosslinked is quite resistant to the diffusion of various ions through it and hence, the time required for reaching equilibrium is much longer. In general, the larger ion or molecule diffusing into an ion exchange particle, or the more highly crosslinked the polymer, the longer the time is required to reach equilibrium conditions.

Copolymers of styrene containing low amounts of divinylbenzene (1-4%) are characterized as having high degree of permeability, large amount of moisture, and high rate to reach equilibrium, but poor physical stability, and selectivity. However, ability to accommodate larger ions is increased. Copolymers of styrene containing high amounts of divinylbenzene (12-16%) exhibit characteristics in the opposite direction.

2.3.3.2 Particle Size

The physical size of the resin particles is controlled during the polymerization step. Screens are used to sieve resins to get a fairly uniform range of sizes. Mesh sizes in Table 2.3 refer to U.S. standard screens. A higher mesh number means more and finer wires per unit area and thus a smaller opening.

Table 2.3 Diameter of particles related to mesh range

Mesh Range	Diameter of Particles (Inches)	Diameter of Particles (Micrometers)
20 - 50	0.0331-0.0117	840-297
50 - 100	0.0117-0.0059	297-149
100 - 200	0.0059-0.0029	149-74
200 - 400	0.0029-0.0015	74-38
minus 400	< 0.0015	< 38

1. Equilibration Rate

The particle size of an ion exchange resin influences the time required to establish equilibrium conditions. There are two types of diffusion that must be considered in an ion exchange equilibrium. The first is called film diffusion or the movement of ions from a surrounding solution to the surface of an ion exchange particle. The second is called internal diffusion which is the movement of ions from the surface to the interior of an ion exchange particle. Film diffusion is usually the controlling reaction in dilute solutions whereas internal diffusion is controlling in more concentrated solutions. The particle size of an ion exchange resin affects both film diffusion and internal diffusion. A fine mesh particle presents more surface area for film diffusion and also contains less internal volume through which an ion must diffuse. A decrease in particle size thus shortens the time required for equilibrium condition.

2. Flow Rate

Ion exchange processes are usually carried out in columns with the resin resting on a suitable support. Liquids may be processed either up-flow or down-flow through such columns. The spherical particles of ion exchange resin resist the flowing of a liquid through or around them. The smaller particle size, the greater this resistance is. This resistance goes up very rapidly when particles smaller than 100 mesh are employed.

2.3.2.3 Pressure Drop

Usually, the resins accede in 1 bar of pressure drop across a bed. The pressure drop is directly proportional not only to the flow rate and the viscosity of the feed, but also the depth of the resin bed, nevertheless is inversely proportional to the square of the diameter of the resin beads. Furthermore, when the resin bed is severely compressed or under high pressure drop (typically beyond 2 or 3 bars depending on the type of resin), the mechanical stress makes the resin likely to be deformed, flattened and ultimately fragmented. Therefore, an operating pressure drop below 1 bar is recommended.

2.4 Zeolite

Zeolites are crystalline aluminosilicates with fully cross-linked open framework structures made up of corner-sharing SiO_4 and AlO_4 tetrahedra. The first zeolite, stibnite, was discovered by Cronstedt in 1756, who found that the mineral loses water rapidly on heating and thus seems to boil. The name “Zeolite” comes from the Greek words zeo (to boil) and lithos (stone). A representative empirical formula of zeolite is $\text{M}_{2/n}.\text{Al}_2\text{O}_3.x\text{SiO}_2.y\text{H}_2\text{O}$, where M represents the exchangeable cation of valence n. M is generally a group I or II ion, although other metal, non-metal and organic cations may also balance the negative charge created by the presence of Al in the structure. The framework may contain cages and channels of discrete size, which are normally occupied by water. In addition to Si^{4+} and Al^{3+} , other elements can also be present in the zeolitic framework. They do not need to be isoelectronic with Si^{4+} and Al^{3+} , but must be able to occupy framework sites. Aluminosilicate zeolites display a net negative framework charge.

2.4.1 Structure of Zeolite

The framework of a zeolite is based on an extensive three-dimensional network in which the polyhedral sites, usually tetrahedral, are linked by oxygen atoms. The crystalline framework contains cages and channels of discrete size and 3-30°A in diameter. The primary building unit of a zeolite is the individual tetrahedral unit. The T atom (T = Si or Al) belonging to a TO_4 tetrahedron is located at each corner, but the oxygen is located near the mid-points of the lines joining each pair of T atoms. The topology of all known zeolite framework types can be described in terms of a finite number of specific combinations of tetrahedral called “secondary building units”(SBU's). A zeolite framework is made up of one type of SBU only.

Description of the framework topology of a zeolite involves “tertiary” building units corresponding to different arrangements of the SBU's in space. Various alternative ways have been proposed. The framework may be considered in terms of large polyhedral building blocks forming characteristic cages. For example, sodalite, zeolite A and zeolite Y can all be generated by the truncated octahedron known as the

beta-cage. An alternative method of describing extended structures uses two-dimensional sheet building units. Sometimes various kinds of chains can be used as the basis for constructing a zeolite framework.

2.4.2 Properties of Zeolite

The most important application of zeolite is used as a catalyst. Zeolites combine high acidity with shape selectivity, high surface area, and high thermal stability and have been used to catalyze a variety of hydrocarbon reactions, such as cracking, hydrocracking, alkylation and isomerisation. The reactivity and selectivity of zeolites as catalysts are determined by the active sites brought about by a charge imbalance between the silicon and aluminium atoms in the framework. Each framework aluminium atom induces a potential active acid site. In addition, purely siliceous and AlPO_4 molecular sieves have Brønsted acid sites whose weak acidity seems to be caused by the presence of terminal OH bonds on the external surface of crystal.

Shape selectivity, including reactant shape selectivity, product shape selectivity or intermedia shape selectivity plays a very important role in zeolite catalysis. The channels and cages in a zeolite are similar in size to medium-sized molecules. Different sizes of channels and cages may therefore promote the diffusion of different reactants, products or intermedia species. High crystallinity and the regular channel structure are the principal features of zeolite catalysts. Reactant shape selectivity results from the limited diffusivity of some of the reactants, which cannot effectively enter and diffuse inside the crystal. Product shape selectivity occurs when slowly diffusing product molecules cannot rapidly escape from the crystal, and undergo secondary reactions. Restricted intermedia shape selectivity is a kinetic effect arising from the local environment around the active site: the rate constant for a certain reaction mechanism is reduced if the necessary intermedia are too bulky to form readily.

Zeolites are selective, high-capacity adsorbents because of their high intracrystalline surface area and strong interactions with adsorbates. Molecules of different size generally have different diffusion properties in the same molecular sieve. Molecules are separated on the basis of size and structure relative to the size

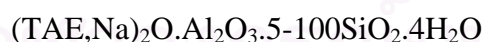
and geometry of the apertures of zeolite. Zeolites adsorb molecules, in particular those with a permanent dipole moments, and exhibit other interactions not found in other adsorbents. Different polar molecules have a different interaction with the zeolite framework, and may thus be separated by a particular zeolite. This is one of the major uses of zeolites. An example is the separation of N₂ and O₂ in the air on zeolite A, by exploiting different polarities of the two molecules.

Zeolites with low Si/Al ratios have strongly polar anionic frameworks. The exchangeable cation creates strong local electrostatic fields and interacts with highly polar molecules such as water. The cation-exchange behaviour of zeolites depends on (1) the nature of the cation species - the cation size (both anhydrous and hydrated) and cation charge, (2) the temperature, (3) the concentration of the cationic species in the solution, (4) the anion associated with the cation in solution, (5) the solvent (most exchange has been carried out in aqueous solutions, although some works have been done in organics) and (6) the structural characteristics of the particular zeolite.

2.4.3 Solid Heterogeneous Catalyst: Beta Zeolite

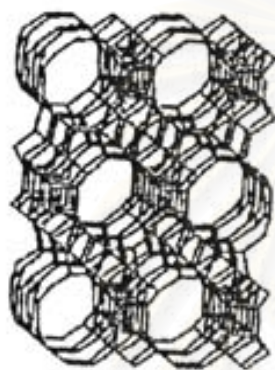
Beta zeolite is an old zeolite discovered before Mobil began the “ZSM” naming sequence. As the name implies, it was the second in an earlier sequence. Beta zeolite was initially synthesized by Wadlinger *et al.* (1995) using tetraethylammonium hydroxide as an organic template.

The chemical composition of beta zeolite is:



Beta zeolite is a large pore, high silica and crystalline aluminosilicate. The framework and the pore structure of the zeolite have several unique features. It is the only large pore zeolite to have chiral pore interactions. The high silica zeolites are attractive catalytic materials because of their thermal and hydrothermal stabilities, acid strength, good resistance for deactivation and hydrophobicity. The pore structure of beta zeolite consists of 12 membered rings interconnected by cages formed by the

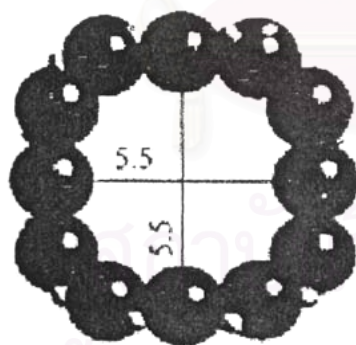
interaction of channels. The dimension of pore opening in the linear channel is $5.7 \text{ \AA} \times 7.5 \text{ \AA}$. The tortuous channel system consists of the interactions of two linear channels of approximate dimensions of $5.6 \text{ \AA} \times 6.5 \text{ \AA}$. Beta zeolite has a total pore volume around 0.2 ml/g . The above characteristics make beta zeolite a potential candidate for a variety of hydrocarbon conversion reactions. The framework structures of beta zeolite are shown in Figure 2.3.



(a) framework structure



(b) framework projection



(c) tortuous channel



(d) straight channel

Figure 2.3 Structure of beta zeolite

2.5 Reactive Distillation

A chemical reaction and multistage distillation can be carried out simultaneously. The combined unit operation, called reactive distillation, especially suits for chemical reactions where reaction equilibrium limits the conversion in a conventional reactor to a low-to-moderate level. By continuously separating products from reactants while the reaction is carried out, the reaction can proceed to much higher level of conversion. Reactive distillation operations are generally used in chemical and petrochemical industry processes to increase product yield.

2.5.1 Reactive Distillation Configurations

A conventional configuration for a chemical process usually involves two steps of chemical reaction and subsequent separation. In the chemical reaction step, reactants are brought into contact with solid catalysts at appropriate process conditions in one or more reactors. The stream leaving the reactor section then goes to one or more separation steps where unconverted reactants are separated from the products of the reaction and the inerts. The unconverted reactants, in some cases, may be recycled to the reaction section. When a substantial amount of inerts are present in the system, at least two separation units for separation of high purity product and for separation of the unconverted reactants from the inerts are required. The separation process in distillations is typically chosen.

A conventional process configuration is shown in Figure 2.4 where a distillation is used for separation. In the case, a reaction product is less volatile than reactants and inert. The flow diagram of the application of reactive distillation to this process is shown in Figure 2.5 The middle section of the column is the reactive distillation section. For a non-azeotropic chemical system, separation of the inerts takes place in the rectification section of the column and the purification of the product takes place in the stripping section.

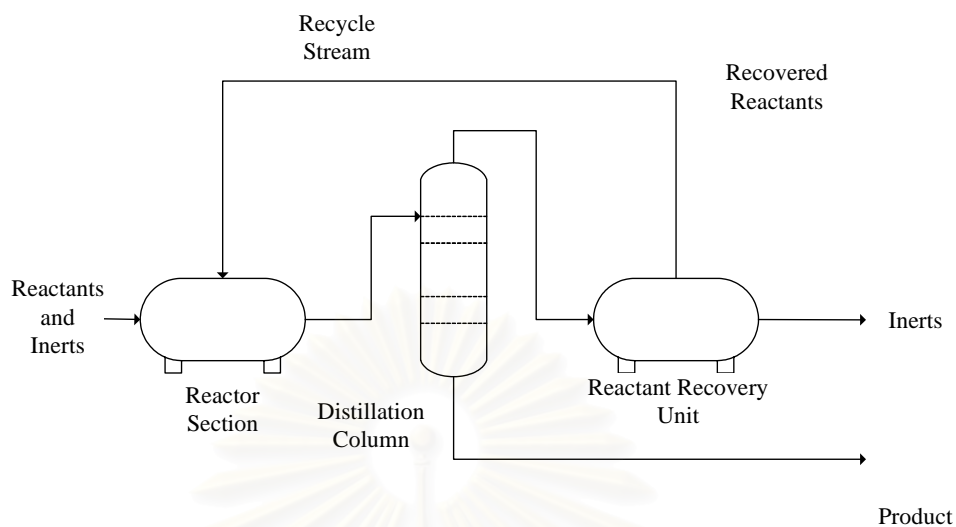


Figure 2.4 Conventional process involving reaction followed by separation

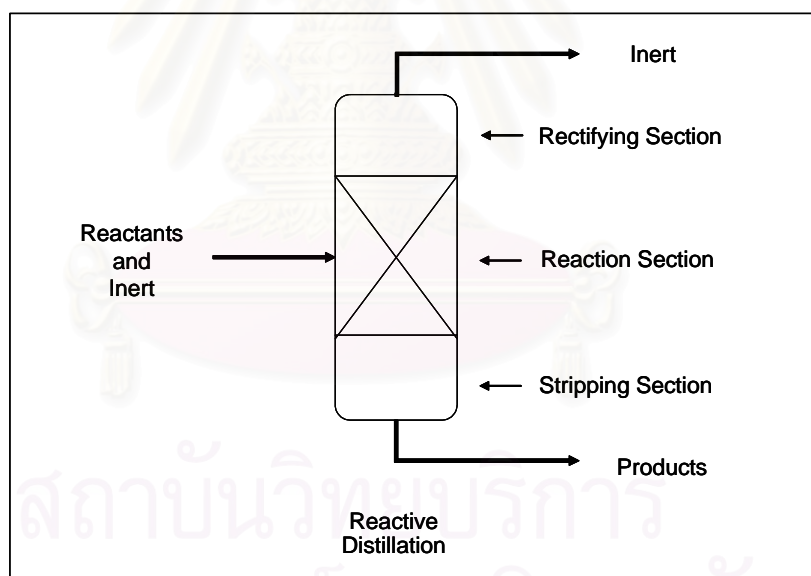


Figure 2.5 Application of reactive distillation for low volatility product process

In the other configuration, the reaction and distillation proceed in alternating steps. The reactive distillation column contains both the catalyst contact device and the distillation device. A reaction occurs in the catalyst contact device and then the reacting phase passes to the distillation device for vapor/liquid contact and separation.

These two steps occur alternately. By making the steps of infinitely small size, this configuration becomes equivalent to the first one. For both configurations, a rectification section may be located above the reactive distillation section of the column and a stripping section may be located below it, depending upon purity specifications.

2.5.2 Advantages of Reactive Distillation

Applications of RD to a catalytic chemical reaction using solid catalysts offer many advantages compared to a conventional process; for example,

1. Two process steps, i.e., separation and reaction, can be carried out in the same device. This integration leads to lower costs in pumps, piping and instrument.
2. The heat released from the reaction can be used for vaporization of liquid. This leads to savings of energy costs by the reduction of reboiler duties.
3. The maximum temperature in the reaction zone is limited to the boiling point of the reaction mixture, so that the danger of hot spot formation on the catalyst is reduced significantly. A simple and reliable temperature control can be achieved.
4. Product selectivity can be improved due to a fast removal of reactants or products from the reaction zone. By this, the probability of consecutive reactions, which may occur in the sequential operation mode, is lowered.
5. If the reaction zone in the RD column is placed above the feed point, poisoning of the catalyst can be avoided. This leads to longer catalyst lifetime compared to conventional systems.

2.6 Aspen Plus

Aspen Plus is one of the components in the Aspen Engineering Suite. It is an integrated set of products designed specifically to promote best engineering practices and to optimize and automate the entire innovation and engineering workflow process throughout the plant and across the enterprise. It automatically integrates process models with engineering knowledge databases, investment analyses, production optimization and numerous other business processes. Aspen Plus contains data, properties, unit operation models, built-in defaults, reports and other features. Its capabilities develop for specific industrial applications, such as petroleum simulation.

Aspen Plus is easy to use, powerful, flexible, process engineering tool for the design, steady-state simulation and optimization of process plants. Process simulation with Aspen Plus can predict the behavior of a process using basic engineering relationships such as mass and energy balances, phase and chemical equilibrium, and reaction kinetic. Given reliable thermodynamic data, realistic operating conditions and the rigorous Aspen Plus equipment models, actual plant behavior can be simulated. Aspen Plus can help to design better plants and to increase profitability in existing plants.

2.6.1 Features of Aspen Plus

1. Utilize the latest software and engineering technology to maximize engineering productivity through its Microsoft Windows graphical interface and its interactive client-server simulation architecture.
2. Contain the engineering power needed to accurately model the wide scope of real-world applications, ranging from petroleum refining to non-ideal chemical systems containing electrolytes and solids.
3. Support scalable workflow based upon complexity of the model, from a simple, single user, process unit flow sheet to a large, multi-engineer developed, multi-engineer maintained, plant-wide flow sheet.

4. Contain multiple solution techniques, including sequential modular, equation-oriented or a mixture of both, and allow as quick as possible solution times regardless of the application.

2.6.2 Benefits of Aspen Plus

1. Proven track record of providing substantial economic benefits throughout the manufacturing life cycle of a process, from R&D through engineering and into production.

2. Allow users to leverage and combine the power of sequential modular and Equation-oriented techniques in a single product, potentially reducing computational times by an order of magnitude while at the same time increasing the functionality and stability of the process model.

3. Complete effectively in an exacting environment to remain competitive in process currently industries it is necessary to do more, often with smaller staffs and more complex process.

CHAPTER III

LITERATURE REVIEWS

Presently, tertiary ethers have become an important additive in gasoline. They are used as octane-enhancing component in gasoline to improve the combustion property of gasoline. Although 2-methoxy-2-methyl propane (methyl tertiary - butyl ether, MTBE) is currently being produced in large scale, the potential risk on the environment and human healthy makes MTBE unattractive. Thus other higher tertiary ethers such as 2-methoxy-2-methylbutane (tertiary-amyl methyl ether, TAME) and 2-ethoxy-2-methylbutane (tertiary-amyl ethyl ether, TAEE) have been of present interest, particularly TAEE. TAEE synthesis is an equilibrium limited reaction and, therefore the conventional reaction and separation processes in single unit operation as reactive distillation has received increasing attention to improve the TAEE synthesis.

The following sections are the literature reviews on production of TAEE from IA and EtOH, and from TAA and EtOH. In addition, application of reactive distillation for the productions of octane-enhancing ether was provided.

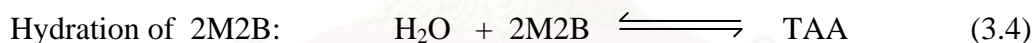
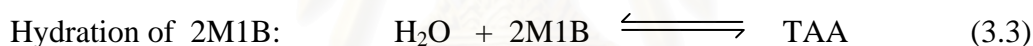
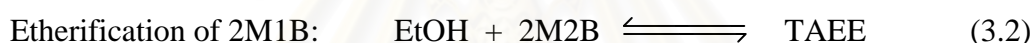
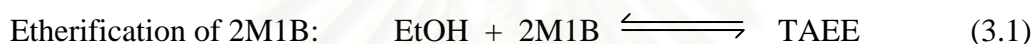
3.1 Production of Tertiary-Amyl Ethyl Ether

The challenges for new routes in the production of higher oxygenate such as ETBE, TAME, and TAEE have been of present interest. However, it is expected that ETBE will face the same problem found in MTBE since it has a similar molecular structure. For this reason, other higher tertiary ethers, e.g. TAME and TAEE are been recently considered to be used as octane enhancing components in gasoline instead of lower ethers. Both of them have lower value of blend Reid vapor pressure; however, the use of TAEE is a more favorable choice compared to TAME. This is attributable to that (1) TAEE has a lower blending Reid vapor Pressure (1.2 psi) than TAME (1.4 psi), (2) the reactants for the production of TAEE can be produced from renewable sources such as cellulose, biomass or other farm products while TAME is

produced from MeOH which seems to be more expensive because it is produced from nonrenewable source, and (3) TAEЕ does not contaminate in underground water. Generally, TAEЕ can be produced from two routes are; i.e. from IA and EtOH, and from TAA and EtOH

3.1.1 Production of TAEЕ from IA and EtOH

The reactions for the synthesis of TAEЕ via IA and EtOH consist of simultaneous etherification (Eqs.3.1 and 3.2), hydration (Eqs. 3.3 and 3.4) and isomerization (Eq.3.5) of the both of isomers of IA; 2 Methyl 1Butene (2M1B) and 2 Methyl 2 Butene (2M2B) as follows:



Several reports for the production of TAEЕ have focused on commercially liquid phase synthesis from EtOH and isoamylene (IA) in many reactors such as; continuous stirred tank reactor, CSTR (Linnekoski et al., 1997, 1998, 1999; Kiviranta-Paakkinen et al., 1998; Oktar et al.,1999b), semi batch reactor (Rihko et al., 1994; Kitchaiya and Datta, 1995; Linnekoski et al., 1998), fixed bed reactor (Boz et al., 2004), plug flow reactor, PFR (Rihko and Krause, 1993). Normally, this etherification can be catalyzed by a strongly acidic macro porous cation-exchange resin, e.g. Amberlyst 15 (Kitchaiya and Datta, 1995; Oktar et al.,1999a, 1999b; Boz et al., 2004 and 2005), Amberlyst 16 (Rihko and Krause, 1993; Rihko et al., 1994, 1997; Linnekoski et al., 1997, 1998, 1999), and Dowex M32 (Rihko and Krause, 1993). These ion exchange resins are formed as an assemble of gel like micro spheres having

macro pores between these micro spheres diffusion resistances. Both in the macro pores and within the gel like micro gains may have significant influence on the observed rate (Oktar et al., 1999a and Dogu et al., 2003). Relative diffusion resistances among macro pores and micro pore are strongly dependent on the state (vapor or liquid) of the reactant. In the liquid phase major diffusion resistance was reported to be in the macro pore (Dogu et al., 2003). However, in vapor phase macro pore and micro pore diffusion resistances are equally significant. Lastly, activity of ion exchange resin, having different hydrogen exchange capacities ranging between 1.3 to 5.1 meq H^+ /kg for TAEЕ synthesis from IA and EtOH was tested in fixed bed reactor (Boz et al., 2004). Amberlyst 15 was prepared with different duration of time for heat treatment at 220 °C. It was observed that even though TAEЕ production from 2M2B increased linearly with an increasing hydrogen ion exchange capacity of catalyst, it became insignificant over a hydrogen ion exchange capacity of 2.8 meq H^+ /kg for TAEЕ production from 2M1B because of its strong influence of diffusion resistance on reaction rate. Furthermore, the diffusion resistances may play an important role on observed rate of TAEЕ synthesis (Oktar et al, 1999b). As a result, the reaction order concentration based of TAEЕ synthesis from 2M1B and 2M2B was not unity, it was 0.93 and 0.69, respectively.

Several research groups have investigated the TAEЕ synthesis from IA and EtOH. Rihko and Krause (1993) published the report for the reactivity of IA with EtOH. It was found that 2M1B was more reactive than 2M2B which is good in agreement with other researches (Oktar et al., 1999b and Boz et al., 2004). Then a number of works have been performed to determine the reaction equilibrium constant and rate expression of the TAEЕ synthesis from IA and ethanol. The equilibrium of TAEЕ synthesis reaction has been studied by Rihko et al. (1994). Likewise, Kitchaiya and Datta, (1995) provided a thermodynamic analysis for equilibrium of simultaneous IA etherification and isomerization reaction. It was found that the observed equilibrium constant corresponded with the thermodynamic value. After that, Linnekoski et al. (1997) studied the simultaneous etherification and hydration of IA and reported that Langmuir-Hinshelwood (L-H) was the best fitted kinetic model among three kinetic models; L-H, Pseudo-Homogeneous, and Eley-Rideal. Subsequently, Linnekoski et al. (1998) published the report of the simultaneous

etherification and hydration reaction of IA. They also focused on water adsorption effect for TAAE formation by using an azeotropic mixture of ethanol and water as reagent using the L-H model as a kinetic model. It was observed that water is the essential inhibitor of TAAE formation. A slight amount of water can largely retard the IA conversion. Then, Linnekoski *et al.* (1999) studied simultaneous etherification and hydration reaction of IA again with various types of alcohol (i.e. methanol, ethanol, and propanol). It was observed that the different kinds of alcohol only affected the isomerization rate but not the etherification rate. Both of the reaction rates are equal until the lowest initial EtOH/2MIB mole ratio reaches 0.2. Whilst, the effect of the alcohol concentration on the side reactions; dialkyl ether formation such as dimethyl ether (DME) and diethyl ether (DEE) were investigated under the temperature varied between 323 and 363 K by Paakkonen *et al.* (1998). It was found that the dialkyl ether formation was preferably performed at high temperature and high alcohol concentration; particularly, DME was formed more than DEE at higher temperature. Moreover, the water produced from dehydration can be further reacted with IA to convert TAA. Recently Boz *et al.* (2005) investigated the mechanism of TAME and TAAE synthesis with diffuse-reflectance FTIR analysis. Although the L-H type model is based on single site adsorption of every component, with the surface reaction being the rate determining step, adsorption equilibrium constant of alcohol was about two order of magnitude greater than IA and TAAE over Amberlyst 15, thus EtOH has significant effect on observed rate when water is absent in this system. The IA hydration has been investigated since 1961 by Odioso *et al.* It was reported that an 30% of conversion of IA to produce TAA as obtained in a fixed bed reactor with a stoichiometric excess of water up to 350%. The result showed a strong equilibrium limitation and also very large mass transfer resistances between the aqueous and organic phases. Subsequently, Delion *et al.* (1987) studied the reaction in an acetone medium, with a large excess of water (about 400%) and Amberlyst-15 catalyst (strongly acidic macroporous resin). A pseudo-first-order dependency of the reaction rate on isoamylene concentration was proposed to fit the data. However, no kinetic or mechanistic interpretation was given. Gonzalez and Fair (1997) determined the best kinetic model from four kinetic models for IA hydration; simple PL model, L-H model, Eley-Rideal, and modified L-H model which considered only water adsorption

over Amberlyst 15. Both forward and backward reactions of the hydration of IA were investigated. It was observed that modified L-H model is the best model to fit the experimental result. Furthermore, it gave the equation of both equilibrium constant and kinetic equation in the expression of Arrhenius's equation and Van' t Hoff equation, respectively which can be employed for kinetic study of TAA dehydration in TAEE synthesis from TAA and EtOH also.

According to the above reports, most of kinetic models take into account the non-ideality of the liquid phase by expression both the reaction equilibrium and the kinetic rate as a function of component activities instead of component concentrations. Thermodynamic calculations were employed to estimate the activity coefficient. The UNIFAC method has been frequently used in the synthesis of TAEE (Paakkinen et al., 1998; Linnekoski et al., 1997, 1998, 1999; Gonzalez and Fair, 1997) compared to the UNIQUAC method (Rihko et al., 1994).

3.1.2 Production of TAEE from TAA and EtOH

Tertiary-amyl alcohol (TAA), one of the major products of fusel oil which is obtained from biomass fermentation, is used as an alternative reactant instead of IA for the synthesis of TAEE (Aiouache and Goto, 2003a). It is the significant choice to reduce economic cost. The reactions are derived from simultaneous etherification (Eq.3.6) and dehydration (Eq.3.7) of TAA converted into TAEE and IA, respectively, while simultaneously, etherification and isomerization of IA can be occurred as showed in Eqs.3.8 and 3.9, respectively.



However, it was found that only a few works have been studied for the synthesis of TAE from TAA and EtOH. For example; Aiouache and Goto (2003a and 2003b) studied the kinetic model of etherification of TAE from TAA and EtOH catalyzed by Amberlyst 15 with the focus on a sorption effect. The results showed that even though the L-H model is more suitable for describing the kinetic of the etherification than simple Power Law model (PL) similarly with TAE synthesis from IA and EtOH, the PL model was useful for modeling of TAE synthesis in reactive distillation using Aspen plus program as simulator in which the PL model based on mole fraction or concentration was required for simulation of RACFRAC column. The study also investigated the effect of feed location and reflux ratio on the performance of reactive distillation inserted by a zeolite Na membrane. After that Sahapatsombud et al (2005) further studied the system of Aiouache and Goto (2003b). The effects of design variables and other operating variables on the performance of reactive distillation were simulated by using Aspen plus program. It was found that the reactive distillation with no rectifying section, 4 stages of reaction section and 8 stages of stripping section is the optimum configuration for TAE synthesis. Further, the reflux ratio and operating pressure are significant factors to operate reactive distillation.

3.2 Application of Reactive Distillation for Octane Enhancing Ether Production

Reactive distillation, an alternative to conventional reactive-separation processes, has received increasing attention in recent years due to its several advantages. For instance, chemical equilibrium limitations can be overcome, higher selectivity can be achieved, heat of reaction can be used in-situ for distillation, auxiliary solvent can be avoided, and azeotropic solutions can be more easily separated. In addition, the most important benefit of reactive distillation is a reduction of capital investment since both chemical reaction and distillation are carried out in the same vessel; one process step is eliminated, along with the associated pumps, piping and instrument (De Garmo et al., 1992). The application of the reactive distillation has been implemented for several reactions for esterification and hydration reaction especially for etherification reaction to produce fuel ethers such as MTBE, ETBE, TAME or TAEF because these reactions are suffered from a chemical-equilibrium limitation (Thiel, et al., 1997).

The first simple reactive distillation was developed in 1921 for the production of methyl acetate. Nowadays, methyl acetate formation in a reactive distillation column is often used to study basic phenomena of the reactive distillation (Bessling et al., 1998). Other esterifications have been studied, such as the esterification of butyl acetate in reactive distillation using Aspen Plus program as simulator by Hanika et al. (1999). It was found that the experimental results are corresponding with simulation results very well. The use of good efficiency of stripping section of the column (at minimum 20 theoretical stage) was achieved to purify butyl acetate from acidic acid. In addition, the result showed that the lower feed rate, the higher conversion.

Recently, reactive distillation is increasingly applied for liquid phase synthesis of octane-enhancing ether. A number of works have investigated the production of MTBE (De Garmo et al., 1992; Jacobs and Krishna, 1993; Nijhuis et al., 1993; Isla and Irazoqui, 1996; Huan et al., 1997; Eldarsi and Douglas, 1998; Higler et al., 1999), the most widely used octane booster for reformulated gasoline, in a RD column. Higler et al. (1999) proposed a non-equilibrium RD model for MTBE synthesis, which was considered as advancement over the pioneering equilibrium model of Jacobs and Krishna (1993).

Recently, there is a pending legislation of the use of MTBE in a number of states in the US due to its tendency to pollute underground water. ETBE is another important oxygenates to replace MTBE. It also shows better blending properties than MTBE. The several researches have been also studied ETBE synthesis in reactive distillation. It was investigated on using reactive distillation for production ETBE from both of direct method by using IB and EtOH as reagents and direct method by using TBA and EtOH as reagents. Almost, many researches focused on EtOH at a concentration low grade until about 2.67 mole% in aqueous phase as low as that obtained from the fermentation of biomass as reported by Roukas (1995). Matouq et al. (1996) studied batch reactive distillation for ETBE synthesis from TBA and low grade alcohol and catalyzed by potassium hydrogen sulfate (KHSO_4). It was observed that ETBE could be produced from these reagents, and reactive distillation was a good choice to separate ETBE from the reagent mixture. Furthermore, Pervaporation was combined with reactive distillation to remove water from the residue product. As a result, the amount of water in the distillate product can be reduced also (Yang and Goto, 1997). Subsequently, Quitain et al. (1999a) studied application of reactive distillation for the ETBE synthesis from TBA and bioethanol (2.5 mol% EtOH in aqueous solution). It was demonstrated that the system could produce 60 mole% ETBE in distillate product while the residue product consisted of mostly water. However, the side reaction of the dehydration of TBA to IB was significant, causing IB-rich gaseous distillate product and low selectivity of ETBE (36 mole %). In addition, they improved the overall selectivity of ETBE by simulating two reactive distillations (Quitain, 1999b). The IB-rich gaseous distillate product from the first reactive distillation column was used to react with pure EtOH in the second reactive distillation column. Certainly, it could increase not only the overall ETBE selectivity up to 99.9%, but also overall conversion of TBA up to 98.9%.

Besides, a dynamic simulation was performed for the ETBE synthesis in the reactive distillation column consisting of 20 stage and five components. The simulations were performed to determine the optimal process condition by using MATLAB simulator (Young et al., 2003).

Although, currently TAEE has gained an increased attention because of its better properties than others there are very limited studies in reactive distillation.

A few reports have been published as Aiouache and Goto (2003b) and Sahapatsombud et al. (2005) have investigated reactive distillation for TAAE synthesis from TAA and EtOH. Furthermore, Varisli and Dogu (2005) considered the simultaneous production of TAAE and TAA from IA-EtOH-water mixtures in a batch reactive distillation. The result was observed that the TAA selectivity is higher than TAAE selectivity. It was due to the higher adsorption equilibrium constant of water than of EtOH over Amberlyst 15. However, when water was not present in system, the 2M2B conversion to TAAE was increased.

Apart from a large number of experimental works on reactive distillation with various reaction systems as mentioned above, modeling and simulation of reactive distillations are a topic of interest over the past years. Many studies have been carried out using a commercial simulation package, e.g., Aspen Plus, Pro/II, HYSYS and SpeedUp. Venkataraman *et al.* (1990) described an inside-out algorithm for calculation in the RADFRAC module of Aspen Plus program. The inside-out methods involves the introduction of new parameters into the model equations and these parameters are used as primary iteration variables. Four case studies reported in their work demonstrated that the RADFRAC can be applied to a wide variety of reactive separation processes with either equilibrium reactions or kinetic-limited reactions. The RADFRAC module has been used to simulate the behavior of a reactive distillation by many authors. For examples, Quitain *et al.* (1999a) simulated a small-scale reactive distillation column in the ETBE production from bioethanol. Later, Quitain *et al.* (1999b) used RADFRAC module to model the reactive distillation in the industrial-scale production of the same process. In addition, Hanika *et al.* (1998) carried out a simulation work on a butylacetate synthesis via catalytic distillation. Furthermore, Smejkal *et al.*, (2001) studied the simulation of 2-Methylpropylacetate synthesis in a system of equilibrium reactor and reactive distillation column. It is noted that all of these studies compared the simulation results computed using Aspen Plus against experimental results and good agreement between experiment and the simulation results was observed.

CHAPTER IV

EXPERIMENT

This chapter describes the experimental procedure for synthesis of the TAE from TAA and ethanol in both semi batch reactor and reactive distillation. It is divided into three parts; catalyst screening, kinetic studies of the dehydration and etherification of TAA, and reactive distillation studies (both experiment and simulation by using Aspen Plus program). Details are given in the following sections.

4.1 Catalyst Screening

4.1.1 Semi Batch Reactor Apparatus

The Autoclave type reactor is cylindrical shape with outside and inside diameter of 5 and 4 cm, respectively and 8 cm of height. It can stand operating pressure as high as 30 atm. The turbine for mixing and valve for liquid sampling including the thermocouple are installed at the top. The mixture was stirred at the maximum speed of 1163 rpm in all the runs to minimize the external mass transfer resistance. Figure 4.1 shows the semi batch reactor apparatus. The experiments carried out at high pressure to ensure all reaction components were always in liquid phase.

สถาบันวิทยบริการ
จุฬาลงกรณ์มหาวิทยาลัย

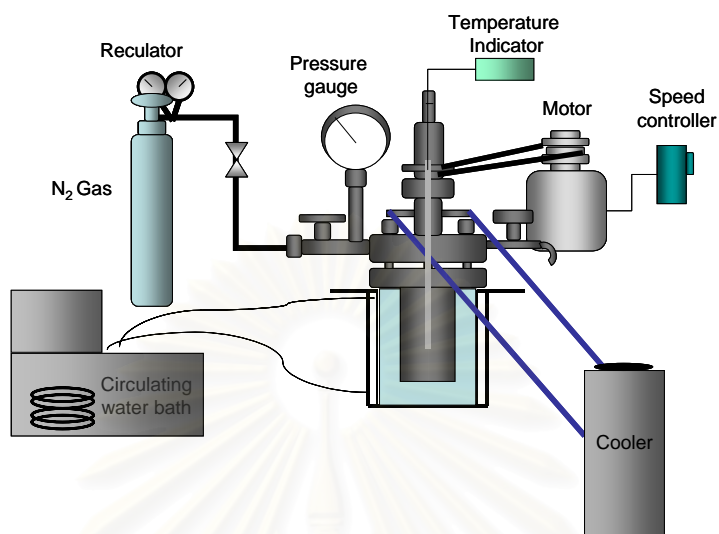


Figure 4.1 Schematic diagram of the catalyst selection experimental set-up

4.1.2 Chemical Materials

The chemicals used in this study consist of standard grade chemicals with purify higher than 99.5% for gas chromatograph calibration and reagent grade chemicals for major experiments. Table 4.1 provides details of the levels of purity and suppliers.

Table 4.1 Details of chemicals use in the study

Chemical materials	Purity (%)	Supplier
Standard grade		
TAA	> 99.6	Chemika Fluka
IA	> 99.5	Chemika Fluka
TAAE	90	Laboratory
Reagent grade		
TAA	96	Chemika Fluka
EtOH	> 99	SR lab

4.1.3 Catalysts

Various commercial catalysts were used in the study as summarized in Table 4.2. It can be divided into 2 types; strong acid ion exchange resin and beta zeolite. Strong acid ion exchange resin can be divided into macroreticular pore and micro pore with styrene-DVB matrix base. The catalysts were dried overnight in an oven at 383 K before use. Furthermore, for beta zeolite with Si/Al ratio of 13.5, it must be ion exchanged to proton form before use (see details in appendix A).

Table 4.2 Various commercial catalysts

Catalysts	Supplier	Ion exchange capacity (meq H ⁺ /kg Catalyst)
Ion exchange Resin		
Macroreticular Pore		
Amberlyst 15	Chemika Fluka	4.7
Amberlyst 16	Chemika Fluka	5.0
Amberlyst 36	Aldrich	5.4
Amberlyst 131	Aldrich	4.8
Micro Pore		
Dowex50wx8	Chemika Fluka	4.8
Zeolite		
β-zeolite with Si/Al = 13.5 (Na ⁺ Form)	Tosoh (Japan)	ND
β-zeolite with Si/Al = 40 (H ⁺ Form)	Tosoh (Japan)	ND

ND = Not Determined

4.1.4 Experimental Procedure

1. 0.6 mol of TAA, 0.6 mol of EtOH and 2g of catalysts were added into the reactor together at room temperature because it did not react at room temperature (Rihko et al., 1998).

2. The solution was pressurized by N₂ gas to 8 atm to prevent vaporization of liquid solutions and heated to the desired reaction temperature (353 K) and stirred at about 1163 rpm.

3. Liquid samples (0.5 cm³) were taken for analysis at 0, 0.25, 0.5, 1, 2, 4, 6, 8, 10, 12 hours. It was noted that, approximately about 1 cm³ of sample was drained before sampling because it had some residue in the sampling part.

4.1.5 Analysis

The analysis was carried out using gas chromatography (GC). The operating condition of the GC is shown in Table 4.3.

An 1x10⁻³ cm³ of sample was injected into the GC and the raw data of chromatograms were modified by using calibration curve (see detail in Appendix B) and were calculated conversion, selectivity and yield to screen the best catalyst for the synthesis TAAE. It should be noted that for experiment with beta zeolite, a sample must be centrifuged before use in order to separate residue catalyst which can damage the GC column.

Table 4.3 Operating conditions of gas chromatography

Gas Chromatography Shimadzu GC8A					
Operating Conditions		Intergration Parameter			
Detector	TCD	Width (sec)	5	Slope (uV/min)	30
Carrier Gas	He (99.98 %)	Drift (uV.min)	0	T. DBL (min)	1000
Carrier Gas Flow rate (cm ³ /min)	30	Stop Time (min)	35	Atten (2 ^X mV)	5
Packed Column	Gaskuropack 54	Speed (mm/min)	2		
Length of Column (m)	2.5			Quantitative Parameters	
Mesh size of Packing	60/80	Method (0-8)	1	Curve (Calib. Fit Type)	0
Injection temperature (K)	443	Cal. Levl (0-15)	1	Min.Area (count)	100
Column temperature (K)	473	Win. Band (0:win 1: Band)	0	Window (%)	5
Detector temperature (K)	473	Spl. Wt	100	IS. Wt	0
Current (A)	80	Dilfact	1		

4.2 Kinetic Study

The major reactions involving in the TAAE synthesis from TAA and EtOH, can be shown below.



TAA etherification (Eq. 4.1) is the major reaction. Simultaneously, TAA can be dehydrated to IA and H₂O according to Eq. 4.2. IA can react with EtOH to produce TAAE (Eq.4.3). The TAA dehydration was investigated first to determine the kinetic parameter of TAA dehydration (k_2) then the TAA etherification was carried out to find the other kinetic parameters. Kinetic was studied on using the same reactor used in the catalyst screening test.

4.2.1 Experimental Procedure of TAA dehydration

1. 0.9 moles of TAA and 2g of selected catalyst were placed into the reactor.
2. The system was pressurized by N₂ gas to 810.4 kPa and heated to the desired temperature of reaction (333, 343 and 353 K) and then stirred at about 1163 rpm.
3. A sample (0.5 cm³) was taken for analysis by GC 8A at 0, 0.25, 0.5, 1, 2, 4, 6, 8, 10, and 12 hours. Approximately 1 cm³ of sample was drained before sampling because it had some residue in the sampling part.

4.2.2 Experimental Procedure of TAA etherification

1. 0.6 moles of TAA and EtOH and 2g of selected catalyst were placed into the reactor.
2. The system was pressurized by N₂ gas to 810.4 kPa and heated to the desired temperature of reaction (333, 343 and 353 K) and then stirred at about 1163 rpm. A sample (0.5 cm³) was taken for analysis by GC 8A at 0, 0.17, 0.33, 0.5, 0.67, 0.83, 1, 2, 4, 6, 8, 10, 12 hours. Approximately 1 cm³ of sample was drained before sampling because it had some residue in the sampling part.

4.2.3 Analysis

The analysis was carried out using a gas chromatography (8A) equivalent to the catalyst screening.

4.3 Reactive Distillation Study

Reactive distillation study is divided into 2 parts; reactive distillation experiment in laboratory and reactive distillation simulation by Aspen Plus Program. The standard operating conditions can be summarized in Table 4.4.

Table 4.4 Standard operating conditions of reactive distillation

Condition of Feed		Column specification	
Temperature (K)	298	Rectifying section (m)	0
Feed flow rate (mole/s)	8.33×10^{-5}	Reaction section (m)	0.19
TAA / EtOH ratio	1	Stripping section (m)	0.31
Mole fraction		Heat duty (watt)	67.5
EtOH	0.5	Catalyst weight (kg)	0.016
TAA	0.5	Reflux ratio	10
Pressure (kPa)	800	Feed stage	2

4.3.1 Reactive Distillation Apparatus

Figure 4.2 shows a schematic diagram of the reactive distillation set-up. It has a four-neck round bottom flask with a mantle heater served as a reboiler. The heat duty at the reboiler was controlled by a valiac. A vacuum-insulated column (inside diameter = 3.5 cm, height = 60 cm) was connected to the central opening of the flask. The column is divided into two sections of reaction and stripping sections. Number of rectifying section is included according to the best column configuration suggested by previous works (Aiouache and Goto, 2003b and Sahapatsombud et al., 2005). About 16 g of catalysts packed in the stainless steel mesh in a shape like tea sack (60 mesh, width = 3 cm, length = 4 cm) were placed inside the column (height = 19 cm) to allow simultaneous reaction and separation of products. Stainless steel mesh saddles (48 mesh, diameter = 3 mm, height = 6 mm) were used as packing materials in the stripping section of the column (height = 31 cm). Six thermocouples were connected along the column height to measure the temperature profiles inside the column. Water at a temperature of 283 K served as a coolant was circulated in the condenser located at the top. The reflux ratio was controlled by the solenoid valve with a multi-timer.

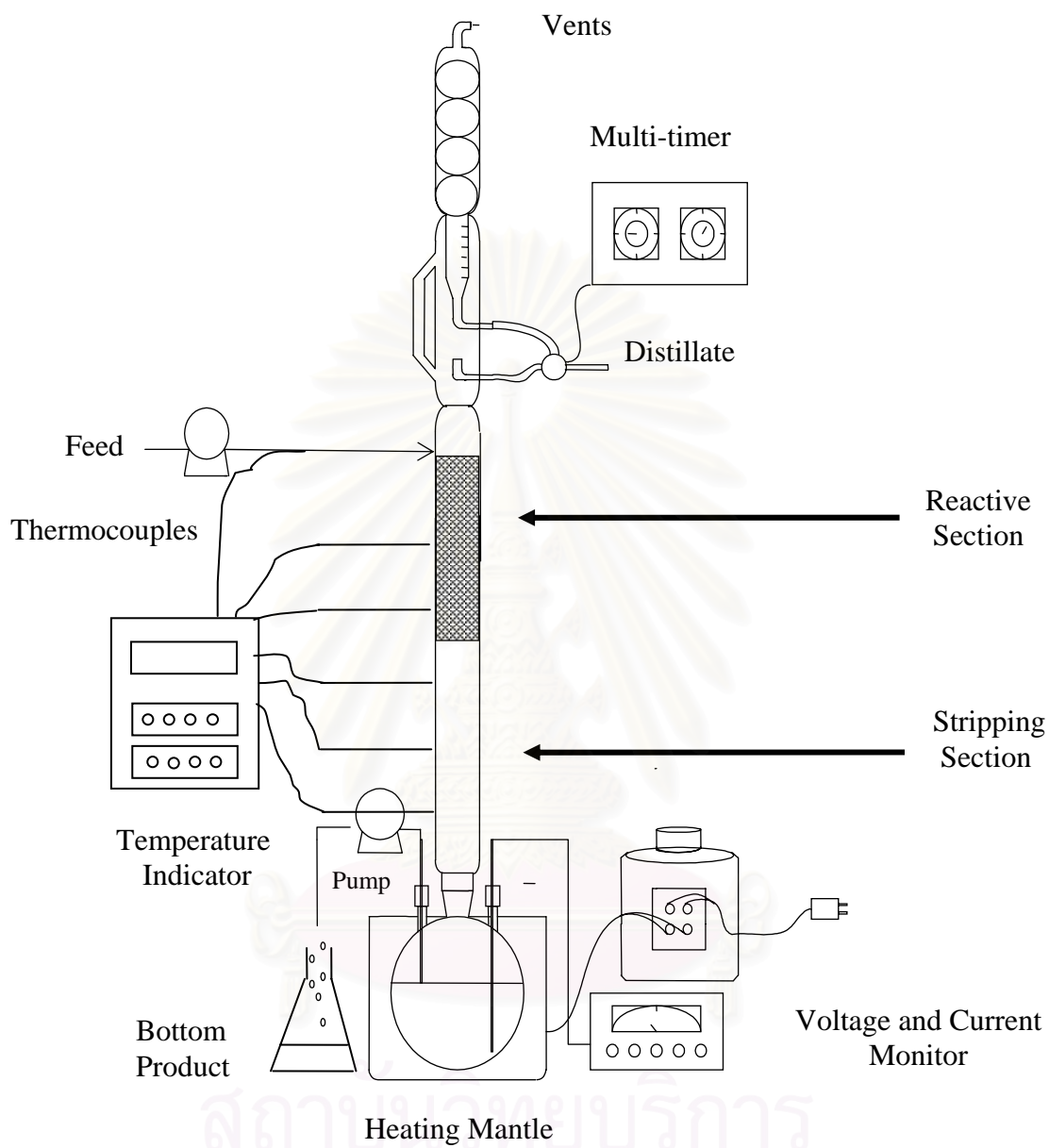


Figure 4.2 Schematic diagram of reactive distillation system

Figure 4.3 shows the configuration of RADFRAC column type reactive distillation for simulation in Aspen Plus program. It consists of 10 stages including the total condenser (stage 1) and the partial reboiler (stage 10). The reaction stage is in the top of column represented by stages 2-5. The feed mixture was fed into the 2nd stage. In the simulation, a property option set PSRK based on the predictive Soave-Redlich-Kwong equation of state was used. The simulation input to Aspen Plus was mainly based on experimental operating condition. The definition of the reflux ratio (L/D) is ratio based on standard volume.

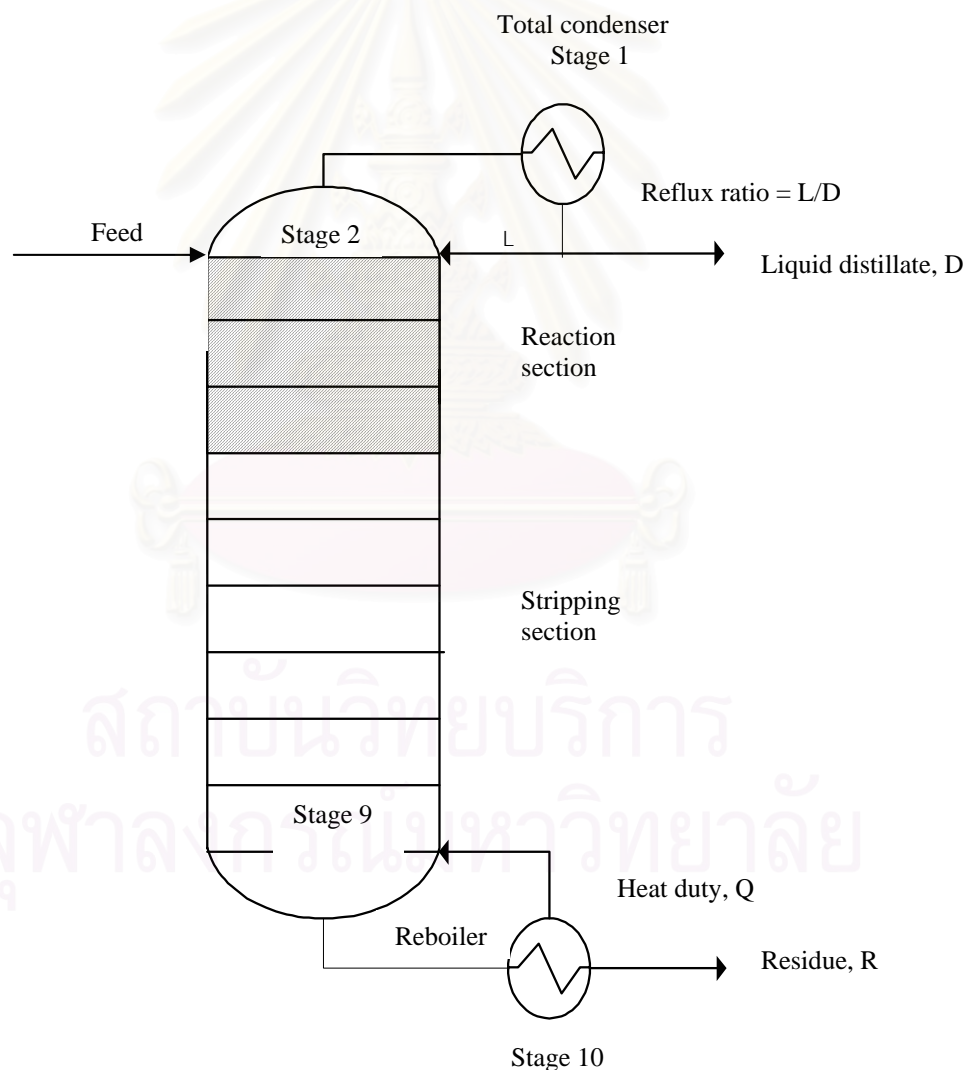


Figure 4.3 Schematic diagram of RADFRAC reactive distillation column

4.3.2. Experiment Procedure of Reactive Distillation

4.3.2.1. Reactive distillation Experiment in laboratory

1. The standard condition of the reactive distillation column was set up.
2. A mixture of 50 cm³ EtOH was placed inside the bottom flask and heated up to boiling point.
3. When first drop of distillate appeared at the top, equimolar feed mixture of TAA and EtOH at room temperature and atmosphere was introduced to the highest part of the reaction section by using a peristaltic pump.
4. Liquid from the reboiler was withdrawn by another peristaltic pump while the distillate was controlled by the reflux ratio. Then, continuous operation was started.
5. The liquid level in the reboiler was maintained by adjusting the tip of the withdrawing pipe connected to the pump.
6. The experiment was conducted for about 12 hours. The distillate and the residue were collected, weighed and analyzed.
7. All steps were repeated with changes in the condition of reflux ratio of 6 and 12, and heat duty of 56 and 93 watt, respectively whereas the other conditions are maintained at the standard conditions to investigate the effect of these parameters.

4.3.2.2. Reactive distillation Simulation by Aspen Plus Program.

1. Set the data of standard condition into program including the kinetic parameters of reaction and run program.
2. Vary input parameters to study the effect of operating parameters on performance of reactive distillation (e.g. reflux ratio, location of feed stage and reaction section, catalyst weight, heat duty, and operating pressure).

4.3.3. Analysis

Reactive distillation performance was considered in terms of conversion of TAA (X_{TAA}), selectivity of TAAE (S_{TAAE}) and yield of TAAE (Y_{TAAE}) as follows;

$$X_{TAA} = \frac{\text{difference in molar flow rate of inlet and outlet of TAA} \times 100}{\text{Molar feed flow rate of TAA}} \quad (4.4)$$

$$S_{TAAE} = \frac{\text{Total Molar flow rate of TAAE in residue and distillate} \times 100}{\text{difference in molar flow rate of inlet and outlet of TAA}} \quad (4.5)$$

$$Y_{TAAE} = \frac{X_{TAA} \times S_{TAAE}}{100} \quad (4.6)$$



สถาบันวิทยบริการ
จุฬาลงกรณ์มหาวิทยาลัย

CHAPTER V

RESULTS AND DISCUSSION

This chapter describes the results and discussion for the synthesis of TAEE from TAA and ethanol in both of semi batch reactor and reactive distillation. It can be divided into three sections; catalyst screening, kinetic study, and reactive distillation study. Details are given in the following section.

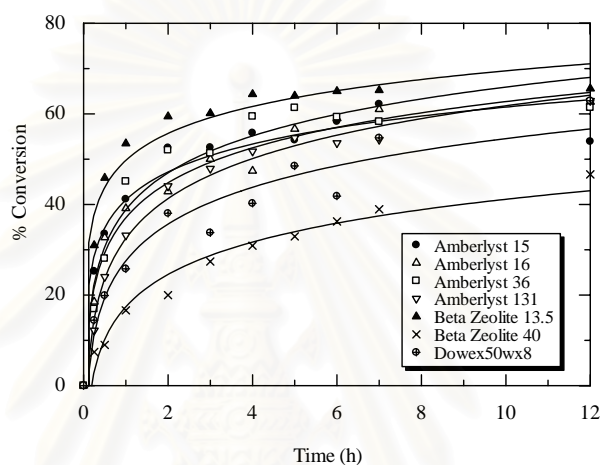
5.1 Catalyst Screening

The catalyst screening experiments were carried out at the following condition; i.e. catalyst weight = 2 g, $T = 353$ K, $P = 810.4$ kPa, maximum turbine speed = 1163 rpm and the initial amount of EtOH and TAA = 0.6 and 0.6 mol, respectively. The reactions taking place in the direct etherification of TAA and EtOH can be summarized as follows;

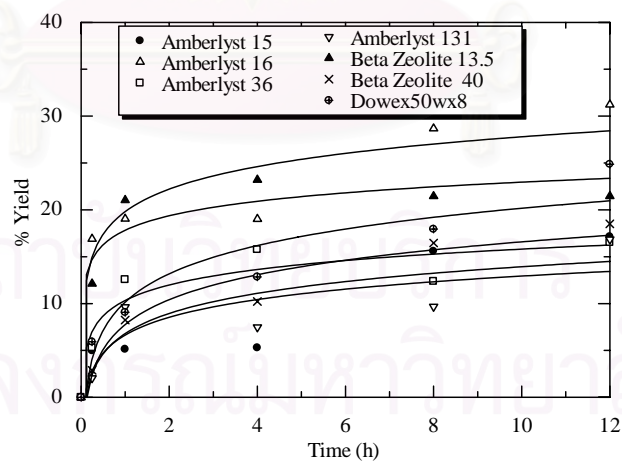


Dehydration of TAA to isoamylene (IA) is a major side reaction; however, IA can further react with EtOH to form TAEE. The catalysts; Amberlyst 15, Amberlyst 16 wet, Amberlyst 36 wet, Amberlyst 131 wet, Beta Zeolite with silica alumina ratio of 13.5 and 40 with H^+ form were screened. The mole to area ratio method and conservative of mass were used for quantitative analysis. TAA conversion and TAEE yield profiles were shown in Figure 5.1(a) and (b), respectively. Their values at 12th hours were summarized in Table 5.1. It was observed that beta zeolite with Si/Al ratio of 13.5 gave the highest conversion (65.6%) while Amberlyst 16 showed the highest selectivity (49.8%) and yield (31.2%). Although a catalyst with high activity and selectivity is a favorable choice for most reactors including reactive distillation,

simultaneous reaction and separation taking place in the reactive distillation allows the system to operate more efficiently and therefore a catalyst with moderate activity can be acceptable. From the obtained results Amberlyst 16 was selected as a suitable catalyst for later investigations in reactive distillation because its selectivity is the highest and its activity is also comparable with that of beta zeolite with Si/Al ratio of 13.5.



(a)



(b)

Figure 5.1 Performances of various catalysts: (a) conversion of TAA, (b) yield of TAEE.

Table 5.1 Summary of performance for various catalysts at 12th hours

Catalysts	% Selectivity of TAAE	% Conversion of TAA	% Yield of TAAE
Amberlyst 15	31.8	53.9	17.1
Amberlyst 16	49.8	62.7	31.2
Amberlyst 36	26.9	61.4	16.5
Amberlyst 131	26.8	62.9	16.9
Beta Zeolite with Si/Al ratio of 13.5	32.7	65.6	21.5
Beta Zeolite with Si/Al ratio of 40	39.7	46.8	18.5
Dowex 50WX8	39.5	62.9	24.9

5.2 Kinetic Study

5.2.1 Development of Mathematical Models

The results from the kinetic study were fitted to two kinetic models; Langmuir-Hinshelwood (L-H) and Power Law model (PL) based on activities (a_i), abbreviated as L-H.A and PL.A, respectively. The L-H model is based on the following assumptions; all components adsorb on the single site of the catalyst and the surface reaction is the rate determining step. According to the previous work of Aiouache and Goto (2003a) it was found from the kinetic study of the same reaction on Amberlyst 15 that the adsorption effect of H₂O and EtOH are stronger than other components. This is also observed by other investigators (Gonzalez and Fair, 1997; Linnekoshi et al., 1997, 1998). As a result, the rate law of all reaction can be expressed in term of activities as

$$r_{1,a} = r_{\text{Etherification of TAA}} = -\frac{k_{1,a} (a_{\text{TAA}} a_{\text{EtOH}} - (1/K_{eq,1a}) a_{\text{TAAE}} a_{\text{H}_2\text{O}})}{(1 + K_{\text{H}_2\text{O},a} a_{\text{H}_2\text{O}} + K_{\text{EtOH},a} a_{\text{EtOH}})^c} \quad (5.4)$$

$$r_{2,a} = r_{\text{Dehydration of TAA}} = -\frac{k_{2,a} (a_{\text{TAA}} - (1/K_{eq,2a}) a_{\text{H}_2\text{O}} a_{\text{IA}})}{(1 + K_{\text{H}_2\text{O},a} a_{\text{H}_2\text{O}})^C} \quad (5.5)$$

$$r_{3,a} = r_{\text{Etherification of IA}} = -\frac{k_{3,a} (a_{\text{IA}} a_{\text{EtOH}} - (1/K_{eq,3a}) a_{\text{TAEe}})}{(1 + K_{\text{H}_2\text{O},a} a_{\text{H}_2\text{O}} + K_{\text{EtOH},a} a_{\text{EtOH}})^C} \quad (5.6)$$

$$C = \begin{cases} 0 & \text{for PL model} \\ 2 & \text{for L-H model} \end{cases}$$

where k_j is the reaction rate constant of reaction j ($j = 1, 2,$ and 3), a_i is an activity of species i , $K_{\text{EtOH},a}$ and $K_{\text{H}_2\text{O},a}$ are the EtOH and H₂O inhibition parameters, and $K_{eq,ja}$ is the equilibrium constant of reaction j expressed as;

$$K_{eq,ja} \equiv \prod_{i=1}^M a_{ie}^{v_{ij}} \quad (5.7)$$

The following expressions of $K_{eq,2a}$ and $K_{eq,3a}$ are adopted from the previous works (Gonzalez and Fair,1997 and Rihko et al., 1994, respectively.)

$$K_{eq,2a} = \exp(10.06 - 3187.4/T) \quad (5.8)$$

$$K_{eq,3a} = \exp(-9.358 + 3283.6/T) \quad (5.9)$$

$$K_{eq,1a} = K_{eq,2a} * K_{eq,3a} \quad (5.10)$$

By performing the material balance for semi batch reactor, the following equations are obtained.

$$\frac{dn_{\text{TAA}}}{dt} = m_r Q_r (-r_1 - r_2) \quad (5.11)$$

$$\frac{dn_{\text{EtOH}}}{dt} = m_r Q_r (-r_1 - r_3) \quad (5.12)$$

$$\frac{dn_{\text{TAEe}}}{dt} = -\frac{dn_{\text{EtOH}}}{dt} \quad (5.13)$$

$$\frac{dn_{\text{H}_2\text{O}}}{dt} = -\frac{dn_{\text{TAA}}}{dt} \quad (5.14)$$

$$\frac{dn_{\text{IA}}}{dt} = \frac{dn_{\text{EtOH}}}{dt} - \frac{dn_{\text{TAA}}}{dt} \quad (5.15)$$

where m_r is weight of catalyst and Q_r is ion-exchange capacity, for Amberlyst 16 is 5.0 meq-H⁺/kg-dry resin.

The activity can be calculated from the following relation.

$$a_i = \gamma_i x_i \quad (5.16)$$

where x_i is mole fraction of species i in the liquid mixture and γ_i is the activity coefficient, can be estimated by using UNIFAC method (see detail in Appendix C).

The reaction rate expressions in term of mole fraction can be defined as follows;

$$r_{1,x} = r_{\text{Etherification of TAA}} = -\frac{k_{1,x} (x_{\text{TAA}} x_{\text{EtOH}} - (1/K_{eq,1x}) x_{\text{TAAE}} x_{\text{H}_2\text{O}})}{(1 + K_{\text{H}_2\text{O},x} x_{\text{H}_2\text{O}} + K_{\text{EtOH},x} x_{\text{EtOH}})^c} \quad (5.17)$$

$$r_{2,x} = r_{\text{Dehydration of TAA}} = -\frac{k_{2,x} (x_{\text{TAA}} - (1/K_{eq,2x}) x_{\text{H}_2\text{O}} x_{\text{IA}})}{(1 + K_{\text{H}_2\text{O},x} x_{\text{H}_2\text{O}})^c} \quad (5.18)$$

$$r_{3,x} = r_{\text{Etherification of IA}} = -\frac{k_{3,x} (x_{\text{IA}} x_{\text{EtOH}} - (1/K_{eq,3x}) x_{\text{TAAE}})}{(1 + K_{\text{H}_2\text{O},x} x_{\text{H}_2\text{O}} + K_{\text{EtOH},x} x_{\text{EtOH}})^c} \quad (5.19)$$

$$\text{where } \left. \begin{aligned} k_{1,x} &= k_{1,a} * (\gamma_{\text{EtOH}} \gamma_{\text{TAA}}) \\ k_{2,x} &= k_{2,a} * (\gamma_{\text{TAA}}) \\ k_{3,x} &= k_{3,a} * (\gamma_{\text{IA}} \gamma_{\text{EtOH}}) \\ K_{eq,jx} &\equiv \prod_{i=1}^M x_{ie}^{v_{ij}} \end{aligned} \right\} \quad (5.20)$$

However, since the activity coefficient of each component is mainly dependent on temperature but less dependent on its composition, the kinetic parameters based on mole fraction can be modified following by the method described in Appendix D.

The temperature dependent rate constant and the chemical equilibrium constant of both models can be expressed by the Arrhenius's equation (Eq.5.21) and the Van't Hoff equation (Eq.5.22), respectively

$$k_j = A_0 \exp\left(\frac{-E_a}{R_g T}\right) \quad (5.21)$$

$$K_{eq,j} = \exp(-\Delta_r G / R_g T) = \exp\left(\frac{-\Delta_r H}{R_g T} + \frac{\Delta_r S}{R_g}\right) \quad (5.22)$$

where E_a is the activation energy (kJ/mole), $\Delta_r H$ is the standard enthalpy change of the reaction, $\Delta_r S$ is standard entropy change of the reaction and R_g is the gas constant.

5.2.2 Kinetic Parameter Determination

5.2.2.1 TAA Dehydration

TAAE synthesis is a complex reaction. It can be directly produced from TAA etherification with EtOH or indirectly from TAA dehydration to IA which further reacts with EtOH to produce TAAE. In this study, the TAA dehydration is firstly investigated to determine the kinetic parameter of this reaction (k_2). Then the TAA etherification is carried out to find the rest kinetic parameters (k_1 and k_3). The reactant of TAA of 0.9 mol was added into the reactor for the TAA dehydration study. The kinetic parameter determination was investigated in the same semi batch reactor used for the catalyst screening at three temperatures 333, 343, and 353 K. Amberlyst 16 (2 g) was used as catalyst. Amberlyst 16 purchased from Fluka has mesh range of 20-50 mesh equivalent to mean particle size diameter of 0.55 mm. According to the

previous work (Rihko et al., 1997), the effect of internal mass transfer can be neglected when using the average particle sizes of Amberlyst 16 of 0.35-0.65 mm while the effect of external mass transfer could be neglected when using the speed of mixing above 300 rpm. The effects of internal and external mass transfer in this study should be small as the catalyst size was in the range reported earlier and the experiments were carried out at high mixing speed (1163 rpm). A MATLAB program was employed to find the best-fitted kinetic parameters which minimize the relative root mean square deviation (RMSD) values expressed by Eq.5.23.

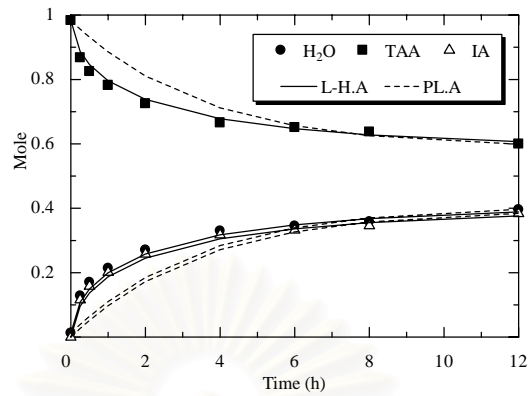
$$RMSD_i = \frac{1}{M} \sqrt{\sum_{K=1}^M \left(\frac{(x_{i,k} - x_{i,exp,k})}{x_{i,exp,k}} \right)^2} \quad (5.23)$$

Figures 5.2. (a), (b) and (c) show the mole profile of each component in the TAA dehydration experiments at 333 343 353 K, respectively. The solid and dashed lines represent the best-fitted simulation results of the L-H.A and PL.A model, respectively. The simulation results of both kinetic models can represent the experimental results quite well. However, the L-H.A model provides better fitting than the PL.A model as also demonstrated by the RMSD values at several temperatures shown in Table 5.2.

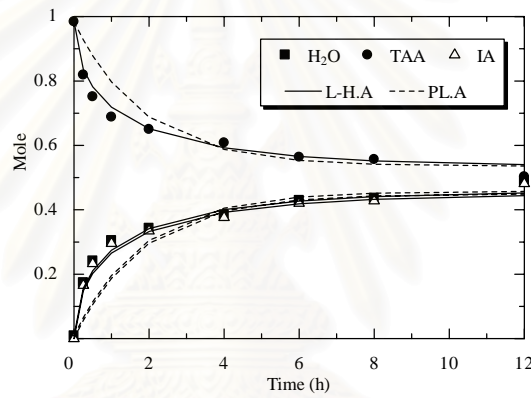
The reaction rate constants at different temperatures were plotted following the Arrhenius's equation as shown in Figure 5.3. The expression of the rate constant and the activation energy for different kinetic models are summarized in Table 5.3.

Table 5.2 RMSD value of kinetic model in each temperature of TAA dehydration reaction

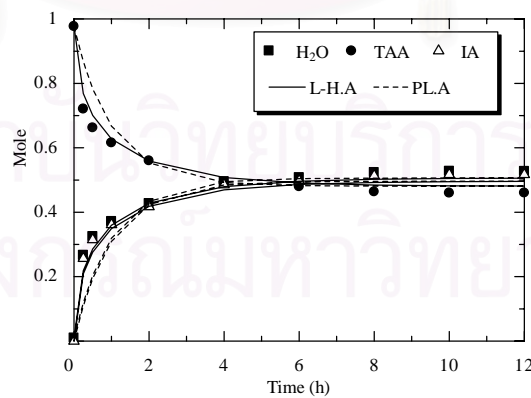
Model	RMSD		
	333K	343K	353K
LH.A	0.012	0.0117	0.0119
PL.A	0.0644	0.0576	0.0368



(a)



(b)



(c)

Figure 5.2 Mole profile of TAA dehydration reaction component ($P = 810.4$ kPa, $m_r = 2$ g, $n_{\text{TAA}} = 0.6$ mole, $n_{\text{EtOH}} = 0.6$ mole): (a) at 333 K, (b) at 343 K, (c) at 353 K (symbols: experiment results, solid lines: L-H.A model, dashed lines: P.L.A model)

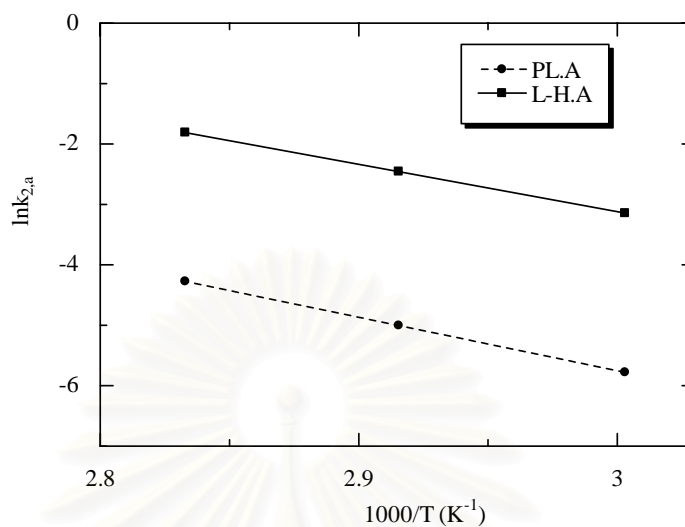


Figure 5.3 Arrhenius's plot of TAA dehydration

Table 5.3 Kinetic constant and activation energy of TAA dehydration

Model	Rate constant (mole/(s*meq H^+))	Activation Energy, E_a (kJ/mole)
L-H.A	$k_2 = \exp(20.4-7840/T)$	65.2
PL.A	$k_2 = \exp(20.77-8840.3/T)$	73.5

สถาบันวิทยบริการ
จุฬาลงกรณ์มหาวิทยาลัย

Besides, the sorption equilibrium constant of H₂O as a function of temperature can be determined by Van't Hoff plot (Figure 5.4) and the expression of Eq.5.23 was obtained. It was found that the value of sorption equilibrium of H₂O decreased with the increase of temperature. This is a conventional behavior observed in most adsorption processes.

$$K_{\text{H}_2\text{O}} = \exp(-2.24+1179/T) \quad (5.23)$$

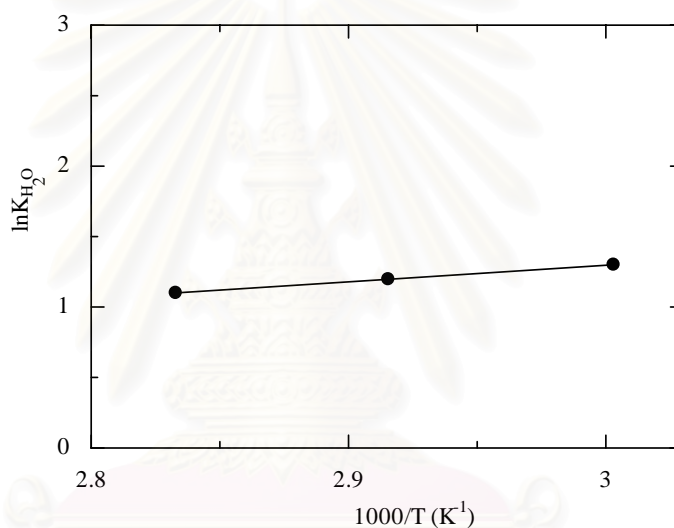


Figure 5.4 Sorption equilibrium constant of H₂O at different temperature

It should be noted that the obtained kinetic parameters of the TAA dehydration were consequently used in the determination of the rest kinetic parameters in the TAA etherification.

5.2.2.2 TAA Etherification

TAA etherification experiment were investigated by using the same semi batch reactor described in the previous TAA dehydration study except that both TAA (0.6 mole) and EtOH (0.6 mole) were reactants.

Figures 5.5 (a), (b) and (c) show the experimental results of mole profile of each component in the TAA etherification at 333, 343 and 353 K, respectively, together with the simulation results from the best-fitted L-H.A, PL.A, and PL.X models. It was found that the experimental results agree well with the simulation results of both kinetic models. As shown in Table 5.4 summarizing the RMSD values of different models, the L-H.A model can describe the rate of TAA etherification better than PL.A model which was also reported by other researches (Linnekoshi et al., 1997, 1998; Gonzalez and Fair, 1997; Aiouache and Goto, 2003a)

Furthermore, the PL model based on mole fraction (PL.X) was considered in this study as it is in a compatible form for use in ASPEN PLUS program. The kinetic parameters of the model can be calculated from the parameters of the activity-based model and average value of activity coefficient for each component. An example of the calculation is given in Appendix D. It was found that the PL.X model can describe the TAA etherification as good as the PL.A model as also shown in Figures 5.5(a), (b) and (c).

Table 5.4 RMSD value of kinetic model in each temperature of TAA etherification reaction

Model	RMSD		
	333K	343K	353K
LH.A	0.028	0.016	0.016
PL.A	0.036	0.024	0.024
PL.X	0.036	0.023	0.023

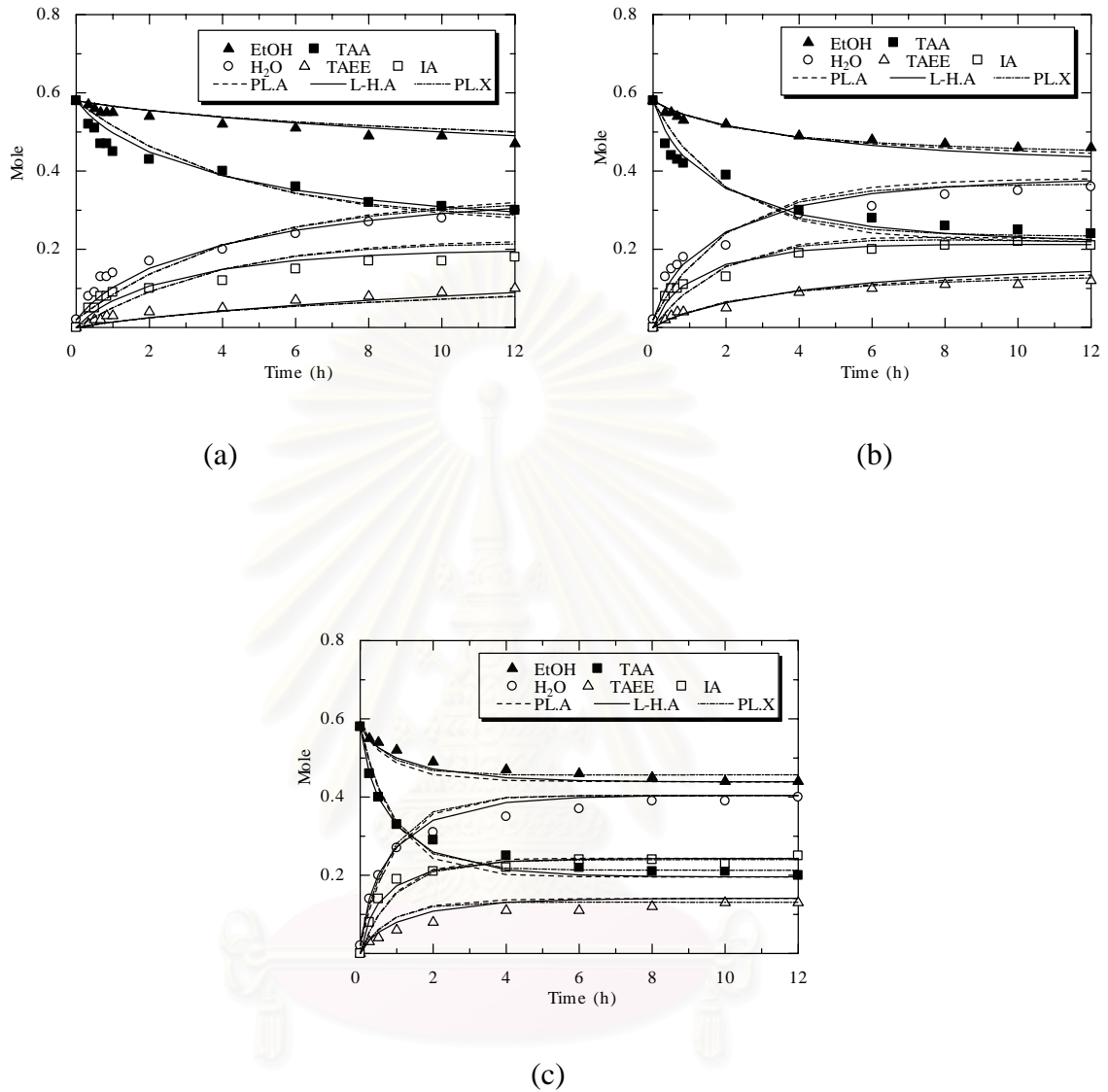


Figure 5.5 Mole profile of TAA etherification reaction component (810.4 kPa, $m_r = 2$ g, $n_{\text{TAA}} = 0.6$ mole, $n_{\text{EtOH}} = 0.6$ mole): (a) at 333 K, (b) at 343 K, (c) at 353 K (symbols: experiment results, solid lines: L-H.A model, dashed lines: PL.A model, and dash dot lines: PL.X model)

The temperature dependent rate constants and sorption equilibrium constants were determined by plotting the relationships according to the Arrhenius' equation (Figure 5.6) and Van't Hoff's equation (Figure 5.7). The expressions of the rate constants and activation energy for different models are summarized in Table 5.5 while the expressions of the sorption equilibrium constants, adsorption enthalpy and adsorption entropy are given in Table 5.6.

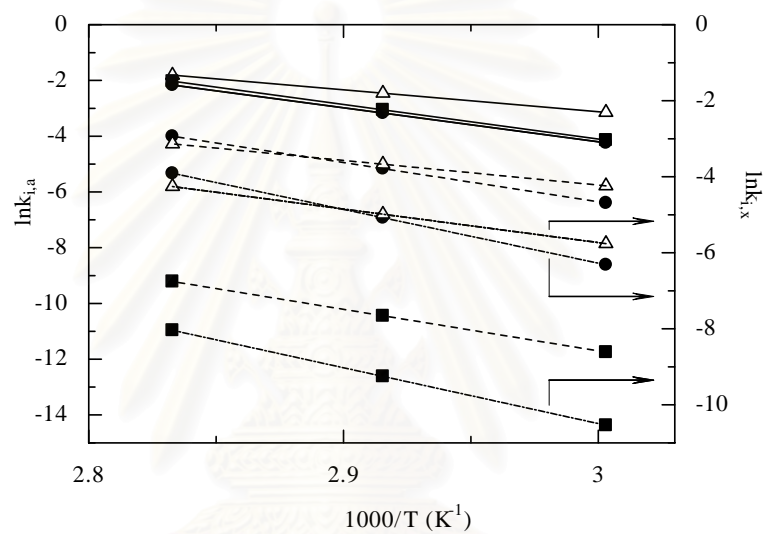


Figure 5.6 Arrhenius's plots (symbols: ● = k_1 , △ = k_2 , ■ = k_3 , dashed lines: PL.A model, solid lines: L-H.A model, and dash dot lines: PL.X model)

สถาบันวิทยบริการ
จุฬาลงกรณ์มหาวิทยาลัย

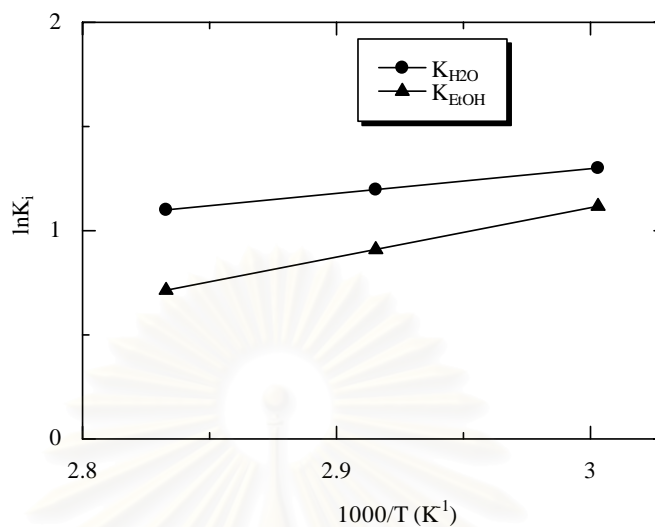


Figure 5.7 Van't Hoff plots for sorption equilibrium constant of H₂O and EtOH

Table 5.5 Reaction rate constants and values of activation energy

Model	Rate Constant (mol/s*meq H ⁺)	Activation Energy, Ea (kJ/mole)
L-H.A	$k_1 = \exp(32.4-12200/T)$	101.4
	$k_2 = \exp(20.4-7840/T)$	65.2
	$k_3 = \exp(33.1-12400/T)$	103.1
PL.A	$k_1 = \exp(35.8-14050/T)$	116.8
	$k_2 = \exp(20.77-8840.33/T)$	73.5
	$k_3 = \exp(33-14900/T)$	123.9
PL.X	$k_1 = \exp(36.154-14142/T)$	117.6
	$k_2 = \exp(20.746-8825.7/T)$	73.4
	$k_3 = \exp(33.577-14690/T)$	122.1

Table 5.6 Sorption equilibrium constant and values of the adsorption enthalpies and adsorption entropies of H₂O and EtOH

Sorption Equilibrium Constant	Enthalpies, ΔH (kJ/mole)	Entropies, ΔS (J/mole*K)
$K_{\text{H}_2\text{O}} = \exp(-2.24+1179/T)$	-9.8	18.6
$K_{\text{EtOH}} = \exp(-6.0+2370/T)$	-19.7	49.9

This comparison of the value of activation energy in all reactions of the TAEE synthesis reported in this work and the literature (Kitchaiya and Datta, 1996; Gonzalez and Fair, 1997; Linnekoshi et al., 1998; Paakkonen et al., 1998; Aiouache and Goto 2003a) is shown in Table 5.7. It was found that the estimated values of activation energy are in acceptable range. A small deviation is due to the difference in reactants and catalyst type.

The sorption equilibrium constant of H₂O and EtOH obtained in this work were compared with that from other researches. It was found that the adsorption enthalpies are similar, but the adsorption entropies are different as shown in Table 5.8. Although our adsorption entropy of EtOH was not equivalent to Linnekoshi et al. (1998), was equivalent to value of Paakkonen et al. (1998) and Aiouache and Goto (2003a).

สถาบันวิทยบริการ
จุฬาลงกรณ์มหาวิทยาลัย

Table 5.7 Comparison the value of activation energy with other researches

Model	Rate constant (mole/s*meq H ⁺)	Activation Energy, E_a (kJ/mole)				
		This work (Amberlyst 16)	Gonzalez and Fair (1997) (Amberlyst 15)	Paakkonen et al. (1998) (Amberlyst 16)	Juha et al. (1998) (Amberlyst 16)	Aiouache and Goto (2003a) (Amberlyst 15)
L-H.A	$K_{1,a}$	101.4	-	-	-	45.1
	$K_{2,a}$	65.2	96.3	-	121.1	45.7
	$K_{3,a}$	103.1	-	95.9	117.7	74
PL.A	$K_{1,a}$	116.8	-	-	-	52.6
	$K_{2,a}$	73.5	105.1	-	-	51.9
	$K_{3,a}$	123.9	-	-	-	76.6

Table 5.8 Adsorption entropies of H₂O and EtOH and values from literature.

Reference	Adsorption entropies (J/(mole K))	
	H ₂ O	EtOH
This work (Amberlyst 16)	19.6	49.9
Linnekoshi et al. (1998) (Amberlyst 16)	25.8	15.2
Aiouache and Goto (2003a) (Amberlyst 15)	29.9	67.3
Paakkonen et al. (1998) (Amberlyst 16)	-	46.4

5.3 Reactive Distillation Study

Both experiment and simulation by using Aspen plus program were carried out to investigate the TAEE synthesis from TAA and EtOH in the reactive distillation. Various operating parameters; i.e. reflux ratio, location of feed stage and reaction section, catalyst weight, heat duty and operating pressure were investigated. The rate expressions obtained from the previous study were important input data for the program. The performance of reactive distillation at standard operating condition was described and then the influence of each operating parameter was discussed.

5.3.1 Performance of Reactive Distillation at Standard Condition

An experiment was carried out at the standard operating condition shown in Table 4.4. The distillate product consists of main reaction product of IA (90 mole%) and small amount of EtOH (7 mole%) and H₂O (1 mole%) while the bottom product consists of the main composition of EtOH (44 mole%), TAA (39 mole%), H₂O (13 mole%), and small composition of TAEE (4%). Table 5.9 compares simulation and experimental results of the distillate and bottom compositions. The program can predict the reactive distillation performances well as good agreement between those results were observed. Figures 5.8 and 5.9 show the mole fraction profiles and temperature profiles of distillate and bottom products, respectively. The dashed lines showed the simulation results from the program. From experimental results, it took around 10 hours to achieve the steady state condition. The corresponding conversion and selectivity at the standard condition were 26.5% (24.7%) and 65.1 % (66.6%), respectively. The values in the parenthesis are those from the simulation.

Table 5.9 Comparison of experimental and simulation results

Components	Distillate (mole fraction)		Bottom (mole fraction)	
	experimental	simulation	experimental	simulation
TAAE	0.00	0.00	0.04	0.08
TAA	0.00	0.02	0.39	0.37
EtOH	0.07	0.10	0.44	0.42
IA	0.92	0.85	0.01	0.00
H ₂ O	0.01	0.02	0.12	0.13
T (K)	314	311	361	357

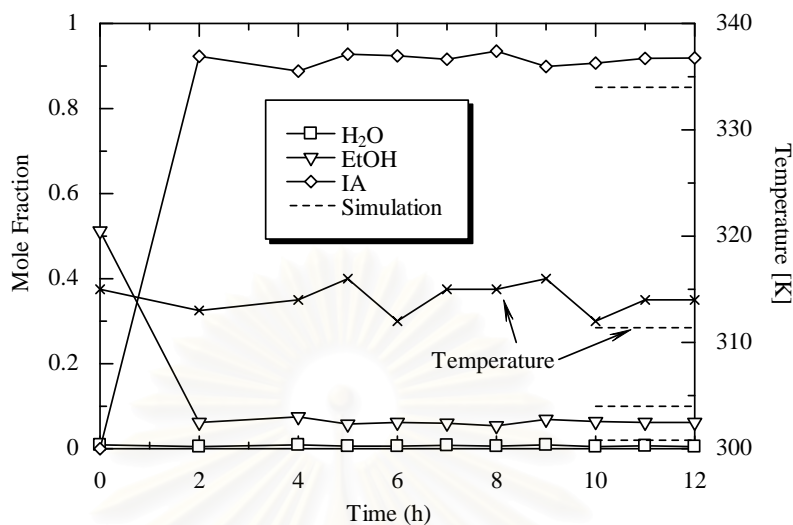


Figure 5.8 Mole fraction profiles and temperature of distillate at standard operating condition (weight of catalyst to feed flow rate ratio = 3.2 kg/(mol/min), reflux ratio = 10, and molar ratio of TAA:EtOH = 1:1)

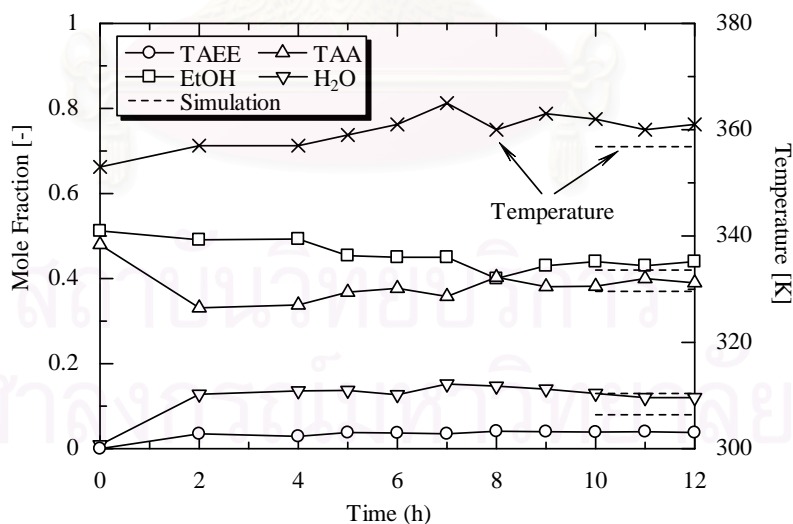


Figure 5.9 Mole fraction profiles and temperature of bottom at standard operating condition (weight of catalyst to feed flow rate ratio = 3.2 kg/(mol/min), reflux ratio = 10, and molar ratio of TAA:EtOH = 1:1)

Figure 5.10 shows the mole fraction and temperature profiles along the column height. The 1st stage is a condenser and the 10th stage is a partial reboiler. Symbols represent the data from experiment. It can be seen that a decrease of TAA mole fraction in the reaction section indicates that the TAA is dehydrated in the upper stage of reaction section (2nd stage) to produce IA while EtOH reacts the etherification reaction in the lower stage of reaction section to convert to TAAE as shown by the slightly increasing mole fraction profile.

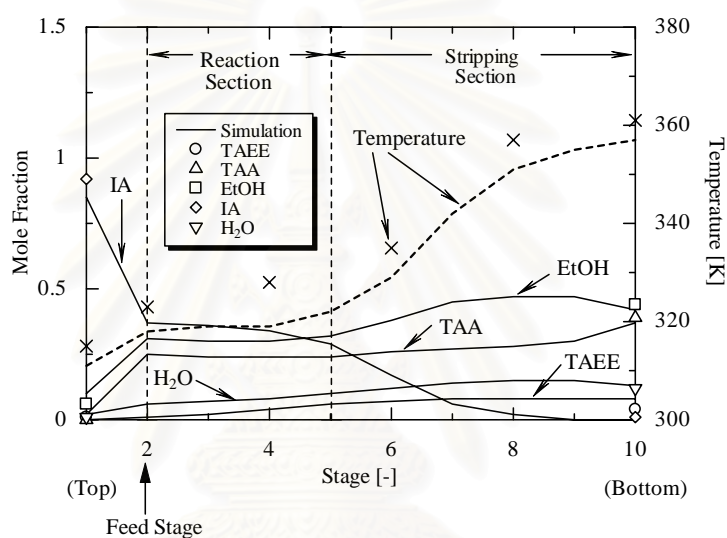


Figure 5.10 Mole fraction and temperature profiles at standard operating condition change with stages (weight of catalyst to feed flow rate ratio = 3.2 kg/(mol/min), reflux ratio = 10, and molar ratio of TAA:EtOH = 1:1)

5.3.2 Effect of Operating Parameters

Aspen Plus program was employed as a main tool to simulate the performance of reactive distillation at various operating parameters. The effects of the reflux ratio, location of feed stage and reaction section, catalyst weight, heat duty and operating pressure were investigated. Due to limitation of the equipment, only some experiments were performed and their results were provided for the main purpose of validation of the simulation results.

5.3.2.1 Effect of Reflux Ratio

Figure 5.11 shows the effect of reflux ratio on the performance of the reactive distillation. The ratio was varied between 2 and 14 while the other operating parameters remained the same as the standard condition. It was found that when the reflux ratio is increased, it does not significantly affect the yield of TAE; however, it has quite pronounced effect on the conversion of TAA and selectivity of TAE. The experimental results (symbols) show good agreement with the simulation results, indicating that the Aspen Plus program can simulate the TAE synthesis in the reactive distillation accurately. When the column is operated at high reflux ratio, more liquid distillate was recycled back to the column and, therefore, the reactant especially ethanol and the product IA can further react within the column. This results in the high selectivity of TAE. However, because the concentration of reactants in liquid phase decreases with the increasing reflux ratio and the column temperature slightly decreases (not shown), the conversion of TAA becomes smaller.

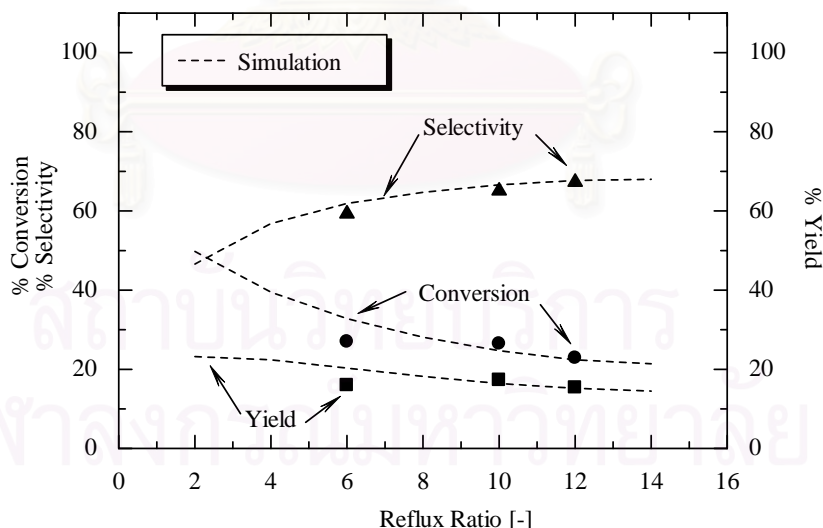


Figure 5.11 Effect of reflux ratio on conversion of TAA, selectivity and yield of TAE (catalyst = Amberlyst 16, catalyst weight to feed flow rate = 3.2 kg/(mole/min), heat duty = 67.5 W, pressure = 101.3 kPa and molar ratio of TAA: EtOH = 1:1)

5.3.2.2 Effect of Location of Feed Stage and Reaction Section

Table 5.10 shows the effect of the location of feed stage and reaction section on the reactive distillation performance. It is noted that F1 is the simulation result at standard condition where the reaction section is represented by stage 2-5, while the feed is introduced at the top of the reaction section (stage 2). By comparing the location of the feed stage (F1-F4), it was found that feeding reactants at the top of the reaction section gives the best reactive distillation performance in terms of the TAA conversion and TAEE selectivity. This may be caused by the decreased residence time of the reactants (TAA and EtOH) as the location of feed is far away from the reaction section. When changing the location of the reaction section (R1-R5), the result showed that the conversion of TAA is increased and the selectivity of TAEE is decreased if the reaction section is more toward the bottom of reactive distillation column. This can be explained by higher temperature in the reaction section; the dehydration of TAA, which is an endothermic reaction, to produce IA is more pronounced; compared to the etherification of TAA to produce TAEE. In addition, although more IA is generated, most of it is in vapor phase because of its lower boiling point and cannot react. As a result, the increased TAA conversion and the decreased TAEE selectivity are observed.

Table 5.10 Effect of location of feed stage and reaction section on conversion of TAA and selectivity of TAEЕ and composition in bottom

Runs	location of feed stage	Reaction section	%Conversion of TAA	%Selectivity of TAEЕ	Composition in bottom				
					TAEЕ	TAA	EtOH	IA	H ₂ O
F1	2	2-5	24.7	66.56	0.08	0.37	0.42	0	0.13
F2	4	2-5	18.88	42.19	0.04	0.4	0.45	0.01	0.1
F3	6	2-5	10.51	17.39	0.01	0.44	0.49	0	0.06
F4	8	2-5	2.07	13.02	0	0.5	0.49	0	0.02
R1	2	3-6	25.54	66.22	0.08	0.37	0.41	0	0.13
R2	2	4-7	27.55	64.74	0.09	0.36	0.41	0.01	0.14
R3	2	5-8	31.57	61.46	0.09	0.33	0.39	0.02	0.16
R4	2	6-9	38.97	54.25	0.1	0.29	0.37	0.04	0.19
R5	2	7-10	54.68	38.78	0.09	0.2	0.35	0.11	0.25

สถาบันวิทยบริการ
จุฬาลงกรณ์มหาวิทยาลัย

5.3.2.1 Effect of Catalyst Weight

Figure 5.12 shows the effect of catalyst weight on performance of reactive distillation, while the other parameters are kept at the standard operating condition. It was found that when the catalyst weight is increased, it does not significantly affect the yield of TAEE; nevertheless, it has an obvious effect on conversion of TAA and selectivity of TAEE. This can be explained that as the catalysts accelerate the TAA etherification reaction to produce TAEE and H₂O, the selectivity of TAEE increases with catalyst weight. However, because of more H₂O occurred in the system, TAA dehydration is shifted backward and therefore, the conversion of TAA was slightly decreased. Although, the increasing of the amount of catalyst weight has a positive effect on the performance of the reactive distillation, other factors, e.g., cost of catalyst and capacity of column, should also be considered in selecting the appropriate amounts of catalyst in the reaction section.

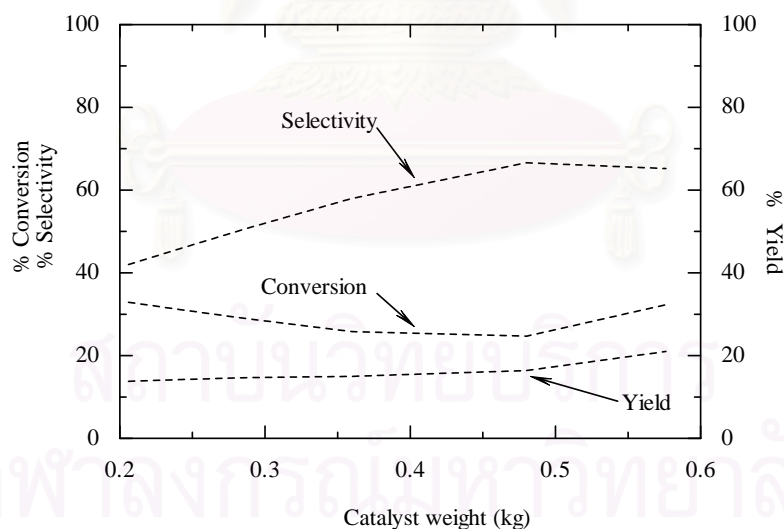


Figure 5.12 Effect of catalyst weight on conversion of TAA, selectivity and yield of TAEE (catalyst = Amberlyst 16, heat duty = 67.5 W, pressure = 101.3 kPa and molar ratio of TAA:EtOH = 1:1)

5.3.2.2 Effect of Heat Duty

Figure 5.13 shows the effect of heat duty on the performance of reactive distillation. The heat duty does not show significant effect on the yield of TAEE at least within the range of study (45-95 W). As the heat duty increases, the conversion of TAA slightly decreases and then increases whereas the selectivity of TAEE decreases from 72.7% to 55.8%. The experimental results (symbols) are in good agreement with the simulation results. At high heat duty, the column is operated at higher vapor-liquid load and temperature. When the reflux ratio is kept unchanged, more reactant especially ethanol is lost from the column as the distillate, leading to the decrease of the selectivity of TAEE. The change in the conversion is mainly governed by the temperature and the liquid concentration in the reaction section which are influenced by the change of heat duty.

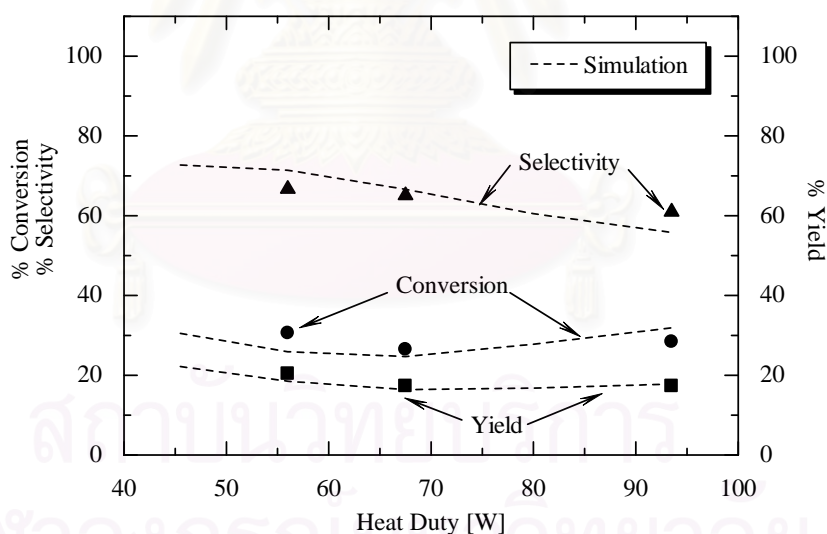


Figure 5.13 Effect of heat duty on conversion of TAA, selectivity and yield of TAEE (catalyst = Amberlyst 16, catalyst weight to feed flow rate = 3.2 kg/(mole/min), heat duty = 67.5 W, pressure = 101.3 kPa and molar ratio of TAA: EtOH = 1:1)

5.3.2.5 Effect of Operating Pressure

The operating pressure is a main factor influencing performance of reactive distillation because it has effect on several properties, for example; the column temperature, reaction temperature system, shifting of boiling point and vaporization of substances including interaction of each component. Figure 5.14 shows the effect of operating pressure on conversion of TAA, selectivity and yield of TAEE. It was observed that operation at 202.6 kPa shows the highest the selectivity and yield of TAEE. When operating pressure is higher than 202.6 kPa, the conversion of TAA increases but the yield of TAEE decreases because the more pronounced decrease of the selectivity of TAEE. As shown in Figure 5.15, operating pressure significantly influences the column temperature profiles. The conversion of TAA increased with the increased operating pressure due to the higher column temperature. Increasing the pressure improves the selectivity of TAEE initially but it becomes worse at higher value. Considering the values of the activation energy of the reactions as shown in Table 5.7, it is expected that the higher operating temperature should improve the reaction selectivity due to the high activation energy of the TAEE synthesis reactions (Eqs. 5.1 and 5.3) compared to that of the TAA dehydration (Eq.5.2). The lower selectivity of TAEE at high operating pressure may be due to the change in vapor-liquid phase equilibrium which is altered by the difference in the column temperature profiles. From this study, the column pressure of 202.6 kPa is the most appropriate condition for the TAEE synthesis.

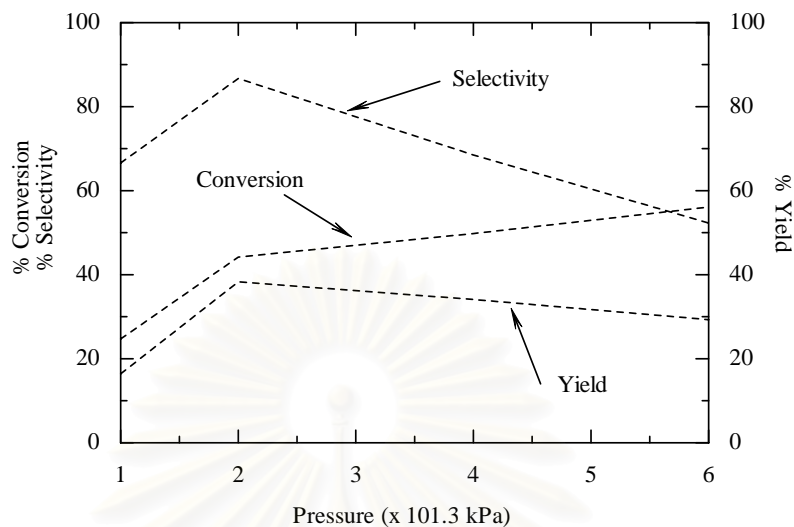


Figure 5.14 Effect of pressure on conversion of TAA, selectivity and yield of TAEE (catalyst = Amberlyst 16, catalyst weight to feed flow rate = 3.2 kg/(mole/min), reflux ratio = 10, heat duty = 67.5 W and molar ratio of TAA: EtOH = 1:1)

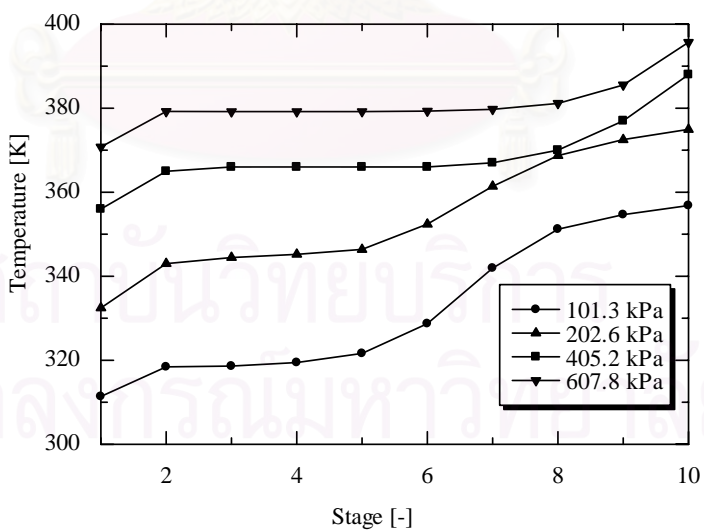


Figure 5.15 Effect of pressure on temperature of each stage (catalyst = Amberlyst 16, catalyst weight to feed flow rate = 3.2 kg/(mole/min), reflux ratio = 10, heat duty = 67.5 W and molar ratio of TAA: EtOH = 1:1)

CHAPTER VI

CONCLUSIONS AND RECOMMENDATIONS

6.1 Conclusions

The application of reactive distillation for production of *tert*- Amyl Ethyl Ether (TAEE) from *tert*- Amyl alcohol (TAA) and ethanol (EtOH) was studied in this thesis. The liquid phase reaction taking place in the reactor systems can be summarized as follows;



The study can be divided into three parts; catalyst screening, kinetic study, and reactive distillation study. The following conclusions can be drawn from the investigations.

6.1.1 Catalyst screening

From the catalyst screening tests using the semi-batch reactor operated at 353 K and 800 kPa. It was observed that Amberlyst 16 is the most attractive catalyst among various tested catalysts (Amberlyst 15, Amberlyst 16, Amberlyst 36, Amberlyst 131, Dowex 50WX8 and beta Zeolite with Si/Al ratio of 13.5 and 40) as it provides the highest selectivity and yield. It was therefore employed in the subsequent studies.

6.1.2 Kinetic study

Amberlyst 16 was employed to study kinetics of TAA dehydration and etherification reaction in the semi-batch reactor at 800 kPa and three temperatures (333, 343, and 353 K). The reactor was operated at the maximum agitation speed (1163 rpm) to avoid the external mass transfer effect and the particle size of catalyst between 0.3-0.8 mm was used in the study. The experimental results were fitted with two activity based kinetic models, Langmuir-Hinshelwood (L-H.A) and Power Law (PL.A). The UNIFAC method was used to estimate the activity coefficient. The L-H model, which is based on single site adsorption of all components and the surface reaction being the rate determining step, is the best kinetic model to fit the experimental data. In addition, PL model based on mole fraction (PL.X) was determined for use in the Aspen Plus program for simulating reactive distillation performance. The model provides equivalent results as calculated by the PL.A model. The Arrhenius 's equations of kinetic rate constant and activation energy for both kinetic models were expressed as;

Model	Rate Constant (mol/s*meq H ⁺)	Activation Energy, E _a (kJ/mole)
L-H.A	$k_1 = \exp(32.4-12200/T)$	101.4
	$k_2 = \exp(20.4-7840/T)$	65.2
	$k_3 = \exp(33.1-12400/T)$	103.1
PL.A	$k_1 = \exp(35.8-14050/T)$	116.8
	$k_2 = \exp(20.77-8840.33/T)$	73.5
	$k_3 = \exp(33-14900/T)$	123.9
PL.X	$k_1 = \exp(36.154-14142/T)$	117.6
	$k_2 = \exp(20.746-8825.7/T)$	73.4
	$k_3 = \exp(33.577-14690/T)$	122.1

In addition, the Van't Hoff equation for chemical equilibrium constant of TAA etherification and sorption equilibrium constant of water and EtOH based on activity can be expressed as;

Chemical Equilibrium Constant	Standard Enthalpies (kJ/mole)
$K_{eq1} = \exp(0.702+96.22/T)$	0.8
$K_{eq2} = \exp(10.06-3187.4/T)$	26.5
$K_{eq3} = \exp(-9.358+3283.62/T)$	27.3

Sorption Equilibrium Constants	Sorption enthalpies (kJ/mole)
$K_{H_2O} = \exp(-2.24+1179/T)$	9.8
$K_{EtOH} = \exp(-6.0+2370/T)$	19.7

6.1.3 Reactive distillation study

Experiments and simulations by using Aspen plus program were carried out to investigate the TAEE synthesis from TAA and EtOH in the reactive distillation. The mole fraction-based PL model obtain from the kinetic study was used to describe the rate expression for TAEE synthesis in Aspen Plus. Various operating parameters; i.e. reflux ratio, location of feed stage and reaction section, catalyst weight, heat duty and operating pressure were investigated.

The result demonstrated that both experiment and simulation results are in good agreement. The distillate product consists of main reaction product of IA 92 mole% (85 mole%) and small amount of EtOH 7 mole% (10 mole%) and H₂O 1 mole% (2 mole%) while the bottom product consists of the main composition of EtOH 44 mole% (42 mole%), TAA 39 mole% (37 mole%), H₂O 12 mole% (13 mole%), and small composition of TAEE 4 mole% (8 mole %). From experimental

results, it took around 10 hours to achieve the steady state condition. The corresponding conversion and selectivity at the standard condition were 26.5% (24.7%) and 65.1 % (66.6%), respectively. The values in the parenthesis are those from the simulation.

Simulation studies of the reactive distillation using Aspen Plus showed that operating pressure and reflux ratio have significant effect on the performance of reactive distillation. From this study, when the reflux ratio is increased, the selectivity of TAEE, also increases, but the conversion of TAA decreases, while when operating pressure are higher than 202.6 kPa, the conversion of TAA increases but the yield of TAEE decreases because of the more pronounced decrease of the selectivity of TAEE. However, the column pressure of 202.6 kPa is the most appropriate condition for the TAEE synthesis

6.2 Recommendations

From experiments of a reactive distillation for the synthesis of TAEE, it was observed that under operating pressure of 101.3 kPa, low selectivity of TAEE was obtained since most TAA was dehydrated to IA and then IA was further reacted with EtOH to produce TAEE. To achieve higher yield of TAEE, the operation of the reactive distillation at higher pressure is preferable. As seen from the simulation studies using the Aspen Plus program; increasing the pressure improved the yield of TAEE. Furthermore, the addition of a pervaporation or membrane system should be alternative route to increase the performance of reactive distillation by separating water, which is the main of inhibitor for this system, promising resulting in higher efficiency TAEE synthesis in reactive distillation.

REFERENCES

- Aiouache, F. and Goto, S. "Sorption effect on kinetics of etherification of *tert*-amyl alcohol and ethanol," *Chemical Engineering Science* 58 (2003a): 2056-2077.
- Aiouache, F. and Goto, S. "Reactive distillation-pervaporation hybrid column for *tert*-amyl alcohol etherification with ethanol," *Chemical Engineering Science* 58 (2003b): 2456-2477.
- Baur, R., Taylor, R. and Krishna, R. "Development of a dynamic nonequilibrium cell model for reactive distillation tray columns," *Chem. Eng. Sci.* 55 (24) (2000): 6139-6154.
- Bessling, B., Loning, J.M., Ohilgslager, A., Schembecker, G. and Sundmacher, K. "Investigation on the Synthesis of Methyl Acetate in a Heterogeneous Reactive Distillation Process," *Chem. Eng. Tech.* 21 (1998): 393-400.
- Boz, N., Dogu, T., Murtezaoglu, K., and Dogu, G. "Effect of hydrogen ion-exchange capacity on activity of resin catalysts in *tert*-amyl ethyl ether (TAE) synthesis," *Applied Catalysis A: General* 268 (2004): 175-182.
- Boz, N., Dogu, T., Murtezaoglu, K., and Dogu, G. "Mechanism of TAME and TAE Synthesis From Diffuse Reflectance FTIR Analysis," *Catalyst Today* 100 (2005): 419-424.
- Collignon, F., Loenders, R., Martens, J.A., Jacobs, P.A. and Poncelet, G. "Liquid Phase Synthesis of MTBE from Methanol and Isobutene Over Acid Zeolites and Amberlyst-15," *Journal of Catalyst* 182 (1999): 302-312.
- Cunill, F., Vila, M., Izquierdo, J.F., Iborra, M., and Tejero, J. "Effect of water Presence on Methyl *tert*- Butyl Ether and Ethyl *tert*-Butyl Ether Liquid-Phase Synthesis," *Ind. Eng. Chem. Res.* 32 (1993): 564-569.
- De Garmo, J.L., Parulekar, V.N., and Pinjala, V. "Consider Reactive Distillation," *Chem. Eng. Prog.* 88 (1992): 43-50.
- Delion, B., Torck, B., and Hellin, M. "Hydration of Isopentenes in an Acetone Environment over Ion-Exchange Resin: Thermodynamic and Kinetic Analysis," *J. Catal.* 103 (1987): 177-187.

- Dogu, T., Aydin, E., Boz, N., Murtezaoglu, K., and Dogu, G. "Diffusion Resistances and Contribution of Surface Diffusion in TAME and TAEE Production Using Amberlyst-15," *Int. J. Chem. React. Eng.* 1 (2003): ArticleA6.
- Donna, L. and Drogos, P.E. "MTBE vs. Other Oxygenates, Mealey's MTBE Conference" (2000).
- Eldarsi, H.S and Douglas, P.L. "Methyl-*tert*-butyl-ether catalytic distillation column-Part I: Multiple steady states," *Chem. Eng. Res. Des.* 76 (A4) (1998): 509-516.
- Gonzalez, J. C., and Fair, J.R. "Preparation of Tertiary Amyl Alcohol in a Reactive Distillation Column. 1. Reaction Kinetics, Chemical Equilibrium, and Mass-Transfer Issues.," *Ind. Eng. Chem.* 36 (1997): 3833-3844 .
- Halim, M.A.A. "The Handbook of MTBE and Other Gasoline Oxygenates," *Marcus Dekker Inc* (2004).
- Hanika, J., Kolena, J. and Smejkal, Q. "Butylacetate via Reactive Distillation-Modelling and Experimental," *Chem. Eng. Sci.* 54 (1999): 5205-5209.
- Hauan, S., Schrans, S. M., and Lien, K. M. "Dynamic Evidence of the Multiplicity mechanism in Methyl *tert*-Butyl Ether Reactive Distillation," *Ind. Eng. Chem. Res.* 36 (1997): 3995-3998.
- Higler, A. P., Taylor, R., and Krishna, R. "Nonequilibrium Modeling of Reactive Distillation: Multiple Steady States in MTBE Synthesis," *Chem. Eng. Sci.* 54 (1999): 1389-1395.
- Isla, M. A., and Irazoqui, H. A. "Modelling Analysis and Simulation of Methyl *tert*-Butyl Ether Reactive Distillation Column," *Ind.Eng. Chem. Res.* 35 (1996): 2696-2708.
- Jacobs, R., and Krishna, R. "Multiple Solutions in Reactive Distillation for Methyl *tert*-Butyl Ether Sythesis," *Ind. Eng. Chem.Res.* 32 (1993): 1706-1709.
- Kitchaiya, P. and Datta, R. "Ethers from Ethanol. 2. Reaction Equilibria of Simultaneous *tert*-Amyl Ethyl Ether Synthesis and Isoamylene Isomerization," *Ind. Eng. Chem. Res.* 34 (1995): 1092-1101.
- Linnekoshi, J.A., Rihko ,L.K. and Krause, A.O.I. "Kinetics of the Heterogeneously Catalyzed Formation of *tert*-Amyl Ethyl Ether," *Ind. Eng. Chem. Res.* 36 (1997): 310-316.

- Linnekoshi, J.A., Rihko, L.K. and Krause, A.O.I. "Etherification and Hydration of Isoamylenes with Ion Exchange Resin," *J. App. Cat A: general.* 170 (1998): 117-126.
- Linnekoski, J.A., Kiviranta-Paakkonen, P. and Krause, O.A. "Simultaneous Isomerization and Etherification of Isoamylenes," *Ind. Eng. Chem. Res.* 38 (1999): 4563-4570.
- Matouq, M, Quitain, A.T., Takahashi, K and Goto, S. "Reactive Distillation for Synthesizing Ethyl *tert*-Butyl Ether from Low-Grade Alcohol Catalyzed by Potassium Hydrogen Sulfate," *Ind.Eng.Chem.Res.* 35 (3) (1996): 982-984.
- Mo, K., Lora, C.O., Wanken, A.E., Javanmardian, M., Yang, N. and Kulpa, C.F. "Biodegradation of Ethyl *tert*-Butyl Ether by Pure Bacterial Cultures," *Appl. Microbiol. Biotechnol.* 47 (1997): 69-72.
- Mohl, K.D., Kienle, A., Gilles, E.D., Rapmund, P., Sundmacher, K. and Hoffmann, U. "Nonlinear dynamics of reactive distillation processes for the production of fuel ethers," *Com.Chem.Eng* 21: (1997): S989-S994 Suppl.
- Nijhuis, S. A., Kerkhof, F. P. J. M., and Mak, A. N. S. "Multiple Steady States during the Reactive Distillation of Methyl *tert*-Butyl Ether," *Ind. Eng. Chem. Res.* 32 (1993): 2767-2774.
- Odioso, R. C., Henke, M., Stauffer, H. C., and Frech, K. J. "Direct Hydration of Olefins with Cation Exchange Resins," *Ind. Eng.Chem.* 53 (3) (1961): 209-211.
- Paakkonen, P.K., Struckmann L.K., Linnekoski, J.A., and Krause A.I.O. "Dehydration of the Alcohol in the Etherification of Isoamylenes with Methanol and Ethanol," *Ind. Eng. Chem.Res.* 37 (1998): 18-24.
- Oktar, N., Murtezaoglu, K., Dogu, T., and Dogu, G. "Dynamic Analysis of Adsorption for ETBE, and TAME Production," *Can. J. Chem. Eng.* 77 (1999a):406-412.
- Oktar N, Murtezaoglu K, Dogu G, Gonderten I, and Dogu T "Etherification Rates of 2-Methyl-2-Butene and 2-Methyl-1-Butene with Ethanol for Environmentally Clean Gasoline Production," *J Chem. Technol. Biot.* 74 (2) (1999b): 155-161.

- Okur, H. and Bayramoglu, M. "The Effect of the Liquid-Phase Activity Model on the Simulation Ethyl Acetate Production by Reactive Distillation," *Ind. Eng. Chem. Res.* 40 (16) (2001): 3639-3646.
- Quitain, A., Itoh, H. and Goto, S. "Reactive Distillation for Synthesizing Ethyl *tert*-Butyl Ether from Bioethanol," *J. Chem. Eng. Japan* 32 (1999a): 280-287.
- Quitain, A., Itoh, H. and Goto, S. "Industrial-Scale Simulation of Proposed Process for Synthesizing Ethyl *tert*-Butyl Ether from Bioethanol," *J. Chem. Eng. Japan* 32 (1999b): 539-543.
- Rihko, L.K. and Krause, A.O.I. "Reactivity of Isoamylene with Ethanol," *J. App. Cat A:general* 101 (1993): 283-295.
- Rihko, L.K., Linnekoshi, J.A. and Krause, A.O.I. "Reaction Equilibria in the Synthesis of 2- Methoxy-2-methylbutane and 2-Ethoxy-2-methylbutane in the Liquid Phase," *J. Chem. Eng. Data* 39 (1994): 700-704.
- Roukas, T. "Ethanol Production from Carob Pod Extract by Immobilized *saccharomyces Cerivisiae* Cells on the Mineral Kissiris," *food Biotechnology(N.Y.)* 9 (1995): 175-178.
- Sahapatsombun, U., Arpornwichanop, A., Assabumrungrat, S., Praserttham P., and Goto, S. " Simulation Studies on Reactive Distillation for Synthesis of *tert*-Amyl Ethyl Ether," *Korean J. Chem. Eng.* 22(3) (2005): 387-392.
- Salanitro, J.P., Diaz, L.A., Williams, M.P. and Wisniewski, H.L. "Isolation of a Bacterial Culture that Degrades MTBE," *Applied Environ. Microbiology* 60 (1994): 2593-2596.
- Smejkal, Q., Hanika, J. and Kolena, J. "2-Methylpropylacetate Synthesis in a System of Equilibrium Reactor and Reactive Distillation Column," *Chem. Eng. Sci.* 56 (2001): 365-370.
- Steffan, R.J., McClay, K., Vaiberg, S., Condee, C.W. and Zhang, D. "Biodegradation of the Gasoline Oxygenates Methyl *tert*-Butyl Ether, Ethyl *tert*-Butyl Ether, *tert*-Amyl Ethyl Ether by Propane-Oxidizing Bacteria," *Applied Environ. Microbiology* 63(11) (1997): 4216-4222.

- Thiel, C., Sundmacher, K., and Hoffmann, U. "Residue Curve Maps for Heterogeneously Catalysed Reactive Distillation of Fuel Ethers MTBE and TAME," *Chem.Eng.Sci.* 52 (6) (1997): 993-1005.
- Tian, Y.C., and Tade, M.O. "Inference of Conversion and Purity for ETBE Reactive Distillation," *Brazilian Journal of Chemical Engineering* 17 (4-7) (2000): 617-625.
- Varisli, D., and Dogu, T. "Simultaneous production of *tert*-Amyl Ethyl Ether and *tert*-Amyl Alcohol from Isoamylene-Ethanol-Water mixtures in a Batch-Reactive Distillation Column," *Ind. Eng. Chem. Res.* 44 (2005): 5227-5232.
- Venkataraman, S., Chan, W.K. and Boston, J.F. "Reactive Distillation Using ASPEN PLUS," *Chem.Eng.Prog* 86 (8) (1990): 45-54.
- Yang, B., and Goto, S. "Pervaporation with Reactive Distillation for the Production of Ethyl *tert*-Butyl Ether." *Sep. Sci. Tech.* 32 (1997): 971-981.
- Yang, B., Yang, S., and Wang, H. "Simulation for the Reactive Distillation Process to Synthesize Ethyl *tert*-Butyl Ether," *J. Chem. Eng. Japan* 34 (2001): 116-1170.
- Yeh, C.K. and Novak, J.T. "Anaerobic Biodegradation of Gasoline Oxygenates in Soils" *Water Environment Research* 66(5) (1994): 744-752.
- Young, H. J. and Tea-Lee, L "Dynamic Simulation for Reactive Distillation with ETBE Synthesis," *Separation and Purification technology* 31 (2003): 301-317.



APPENDICES

สถาบันวิทยบริการ
จุฬาลงกรณ์มหาวิทยาลัย

APPENDIX A

PRETREATMENT PROCEDURE OF BETA ZEOLITE WITH Si/Al RATIO OF 13.5

1. Ammonium Ion-Exchange

The ion-exchange step was carried out by mixing the Na⁺ beta Zeolite with Si/Al ratio of 13.5 in 2 M NH₄NO₃ (ratio of catalyst and solution is 1g:30 cm³) using a stirring hot plate at 353 K for 1 hour. The mixture was cooled down to room temperature. Then, the ion-exchanged crystals were washed twice with de-ionized water by using a centrifugal separator. After that, the ion-exchanged crystals were dried at 383 K for at least 180 minutes in the oven. The dried crystals (NH₄- beta zeolite) were obtained.

2. Second Calcination

The removable species, i.e. NH₃ and NO_x were decomposed by thermal treatment of the ion-exchanged crystals in a furnace by heating them from the room temperature to 773 K in 1 hour in air stream and maintained at this temperature for 2 hours. After this step, the obtained crystals were H⁺-beta zeolite which was used for kinetic study.

APPENDIX B

CALIBRATION CURVE

The calibration curves of all components involving in the reaction system were prepared. The thermal conductivity detector, gas chromatography Shimadzu model 8A equipped with gaskuropack 54 column was used to analyze the quantity of all components. The chromatograms of all components; TAA, EtOH, IA, H₂O and TAAE are demonstrated in relationship between area and retention time as showed in Figure B.1 and the calibration curves of all components in relationships between mole and area are obtained as Figure B.2.

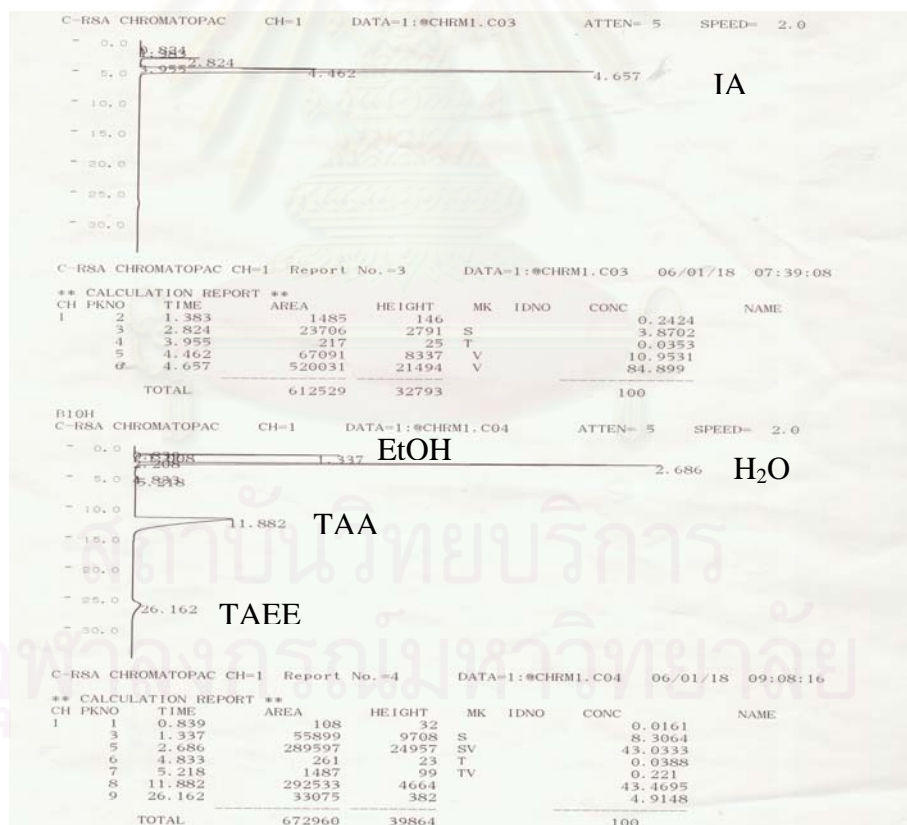


Figure B.1 Chromatograms of all components in TAAE synthesis system (integration parameters: width = 5 sec, stop time = 35 min, speed = 2 mm/min, slope = 30 uV/min, atten = 5 mV, min. area = 100 count)

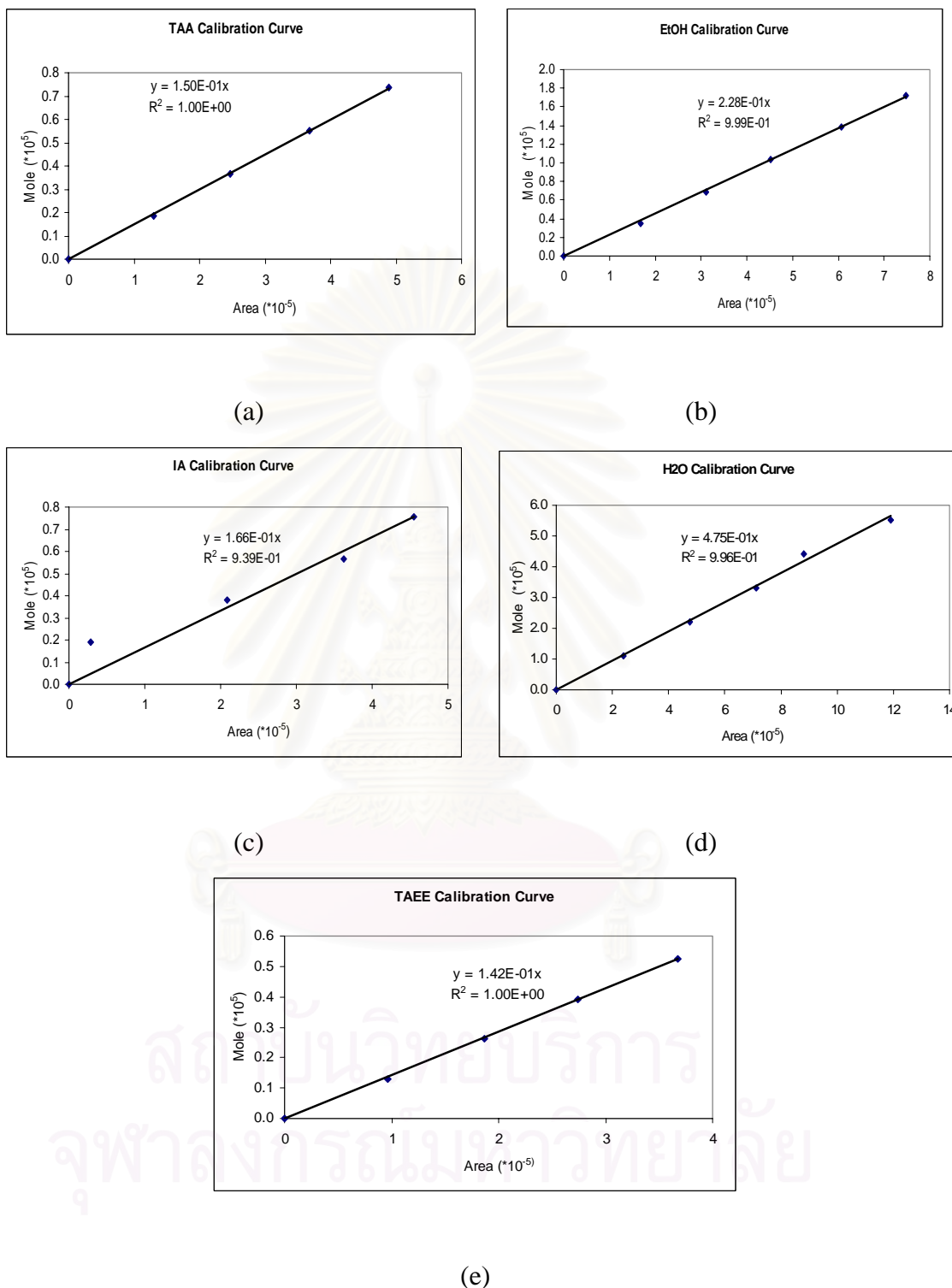


Figure B.2 Calibration curves of all components in TAAE synthesis system

(a) TAA, (b) EtOH, (c) IA, (d) H₂O and (e) TAAE

APPENDIX C

UNIFAC METHOD

Basic Background

The UNIFAC (UNIQUAC Functional-group Activity Coefficients) method for estimation of liquid-phase activity coefficient is based on the concept that a liquid mixture may be considered as a solution of the structural units from which the molecules are formed rather than a solution of the molecules themselves. These structural units are called subgroups, and some of them are listed in the second column of Table C.1. A number, designated k , identifies each subgroup. The relative volume R_k and relative surface area Q_k are properties of the subgroups, and values are listed in column 4 and 5 of Table C.1. When it is possible to construct a molecule from more than one set of subgroups, the set containing the least member of different subgroups is the correct set. The great advantages of the UNIFAC method are;

1. Theory is based on the UNIQUAC method.
2. Parameters are essentially independent of temperature.
3. Size and binary interaction parameters are available for wide range of types of functional groups.
4. Prediction can be made over a temperature range of 275 to 425 K and for pressure up to a few atmospheres.
5. Extensive comparisons with experimental data are available.

Activity coefficients depend not only on the subgroup properties R_k and Q_k , but also on interactions between subgroups. Here, similar subgroups are assigned to a main group, as shown in the first two columns of Table C.1. The designations of main groups, such as “CH₂”, “ACH”, etc., are descriptive only. All subgroups belonging to the same main group are considered identical with respect to group interactions. Therefore parameters characterizing group interactions are identified with pairs of main groups. Parameter value a_{mk} for a few such pairs are given in Table C.2.

The UNIFAC method is based on the UNIQUAC equation which treats $g \equiv G^E / RT$ as comprised of two additive parts, a *combinatorial* term g^C to account for molecular size and shape differences, and a *residual* term g^R to account for molecular interactions:

$$g = g^C + g^R \quad (\text{C-1})$$

The function g^C contains pure-species parameters only, whereas the function g^R incorporates two binary parameters for each pair of molecules. For a multi-component system,

$$g^C = \sum x_i \ln \frac{\phi_i}{x_i} + 5 \sum q_i x_i \ln \frac{\theta_i}{\phi_i} \quad (\text{C-2})$$

and

$$g^R = - \sum q_i x_i \ln (\sum \theta_j \tau_{ji}) \quad (\text{C-3})$$

where

$$\phi_i = \frac{x_i r_i}{\sum x_j r_j} \quad (\text{C-4})$$

and

$$\theta_i = \frac{x_i q_i}{\sum x_j q_j} \quad (\text{C-5})$$

Subscript i identifies species, and j is a dummy index; all summations are over all species. Note that $\tau_{ji} \neq \tau_{ij}$; however, when $i = j$, then $\tau_{ji} = \tau_{ij} = 1$. In these equations, r_i (a relative molecular volume) and q_i (a relative molecular surface area) are pure-species parameters. The influence of temperature on g enters through the interaction parameters τ_{ji} of Eq. (C-3), which are temperature dependent:

$$\tau_{ji} = \exp \frac{-(u_{ji} - u_{ii})}{RT} \quad (\text{C-6})$$

Parameters for the UNIQUAC equation are therefore values of $(u_{ji} - u_{ii})$.

Calculation of Activity Coefficient

An expression for $\ln \gamma_i$ is applied to the UNIQUAC equation for g [Eqs. (C-1) through (C-3)]. The result is given by the following equations:

$$\ln \gamma_i = \ln \gamma_i^C + \ln \gamma_i^R \quad (\text{C-7})$$

$$\ln \gamma_i^C = 1 - J_i + \ln J_i - 5q_i \left(1 - \frac{J_i}{L_i} + \ln \frac{J_i}{L_i}\right) \quad (\text{C-8})$$

and

$$\ln \gamma_i^R = q_i \left(1 - \ln s_i - \sum \theta_j \frac{\tau_{ij}}{s_j}\right) \quad (\text{C-9})$$

where

$$J_i = \frac{r_i}{\sum x_j r_j} S \quad (\text{C-10})$$

$$L_i = \frac{q_i}{\sum x_j q_j} S \quad (\text{C-11})$$

$$s_i = \sum \theta_l \tau_{li} \quad (\text{C-12})$$

Again, subscript i identifies species, and j and l are dummy indices. All summations are over all species, and $\tau_{ij}=1$ for $i=j$. Values for the parameters $(u_{ij} - u_{jj})$ are found by regression of binary VLE data.

When applied to a solution of groups, the activity coefficients are calculated by:

$$\ln \gamma_i = \ln \gamma_i^C + \ln \gamma_i^R \quad (\text{C-13})$$

when

$$\ln \gamma_i^C = 1 - J_i + \ln J_i - 5q_i \left(1 - \frac{J_i}{L_i} + \ln \frac{J_i}{L_i}\right) \quad (\text{C-14})$$

and

$$\ln \gamma_i^R = q_i \left[1 - \left(\theta_k \frac{\beta_{ik}}{s_k} - e_{ki} \ln \frac{\beta_{ik}}{s_k}\right)\right] \quad (\text{C-15})$$

The quantities J_i and L_i are given by:

$$J_i = \frac{r_i}{x_j r_j} \quad (\text{C-16})$$

$$L_i = \frac{q_i}{x_j q_j} \quad (\text{C-17})$$

In addition, the following definitions of parameters in Eqs. C-14 and C-15 are applied:

$$r_i = v_k^{(i)} R_k \quad (\text{C-18})$$

$$q_i = v_k^{(i)} Q_k \quad (\text{C-19})$$

$$e_{ki} = \frac{v_k^{(i)} Q_k}{q_i} \quad (\text{C-20})$$

$$\beta_{ik} = e_{mi} \tau_{mk} \quad (\text{C-21})$$

$$\theta_{ik} = \frac{x_i q_i e_{ki}}{x_j q_j} \quad (\text{C-22})$$

$$s_k = \theta_m \tau_{mk} \quad (\text{C-23})$$

$$\tau_{mk} = \exp\left(\frac{-a_{mk}}{T}\right) \quad (\text{C-24})$$

Subscript i identifies species, and j is a dummy index running over all species. Subscript k identifies subgroups, and m is a dummy index running over all subgroups. The quantity $\nu_k^{(i)}$ is the number of subgroups of type k in a molecule of species i . Values of the subgroup parameters R_k and Q_k and of the group interaction parameters, a_{mk} come from tabulation in the literature. Tables C.1 and C.2 shown some parameter values.



สถาบันวิทยบริการ
จุฬาลงกรณ์มหาวิทยาลัย

Table C.1 UNIFAC-VLE subgroup parameters[†]

Main group	Subgroup	Group name	Rk	Qk
1	1	CH ₃	0.9011	0.848
1	2	CH ₂	0.6744	0.540
1	3	CH	0.4469	0.228
1	4	C	0.2195	0.000
2	5	CH ₂ =CH	1.3454	1.176
2	6	CH=CH	1.1167	0.867
2	7	CH ₂ =C	1.1173	0.988
2	8	CH=C	0.8886	0.676
2	9	C=C	0.6605	0.485
3	10	ACH	0.5313	0.400
3	11	AC	0.3652	0.120
4	12	ACCH ₃	1.2663	0.968
4	13	ACCH ₂	1.0396	0.660
4	14	ACCH	0.8121	0.348
5	15	OH	1.0000	1.200
6	16	CH ₃ OH	1.4311	1.432
7	17	H ₂ O	0.9200	1.400
8	18	ACOH	0.8952	0.680
9	19	CH ₃ CO	1.6724	1.488
9	20	CH ₂ CO	1.4457	1.180
10	21	CHO	0.9980	0.948
11	22	CH ₃ COO	1.9031	1.728
11	23	CH ₂ COO	1.6764	1.420
12	24	HCOO	1.2420	1.188
13	25	CH ₃ O	1.1450	1.088
13	26	CH ₂ O	0.9183	0.780
13	27	CH-O	0.6908	0.468
13	28	FCH ₂ O	0.9183	1.100
14	29	CH ₃ NH ₂	1.5959	1.544
14	30	CH ₂ NH ₂	1.3692	1.236
14	31	CHNH ₂	1.1417	0.924
15	32	CH ₃ NH	1.4337	1.244
15	33	CH ₂ NH	1.2070	0.936
15	34	CHNH	0.9795	0.624
16	35	CH ₃ N	1.1865	0.940
16	36	CH ₂ N	0.9597	0.632
17	37	ACNH ₂	1.0600	0.816
18	38	C ₃ H ₅ N	2.9993	2.113
18	39	C ₃ H ₄ N	2.8332	1.833
18	40	C ₃ H ₃ N	2.6670	1.553
19	41	CH ₃ CN	1.8701	1.724
19	42	CH ₂ CN	1.6434	1.416
20	43	COOH	1.3013	1.224
20	44	HCOOH	1.5280	1.532
21	45	CH ₂ Cl	1.4654	1.264
21	46	CHCl	1.2380	0.952
21	47	CCl	1.0060	0.724

[†] Adapted from xLUNIFAC Version 1.0

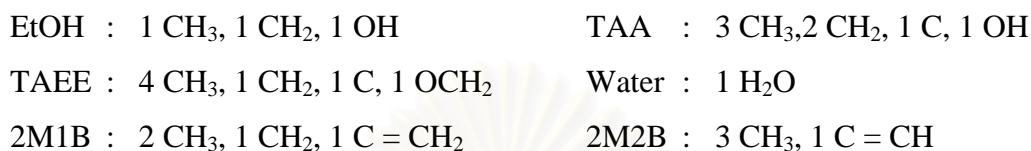
Table C.2 UNIFAC-VLE group interaction parameters, a_{mk} , in Kelvins[†]

a_{mk}	k	1	2	3	4	5	6	7	8	9	10	11	12	13	14	15	16	17	18	19	20
m	Name	CH ₂	C=C	ACH	ACCH ₂	OH	CH ₃ OH	H ₂ O	ACOH	CH ₂ CO	CHO	CCOO	HCOO	CH ₂ O	CNH ₂	CNH ₂	(C) ₃ N	ACNH ₂	PYRIDINE	CCN	COOH
1	CH ₂	0	86.02	61.13	76.5	986.5	697.2	1318	1333	476.4	677	232.1	741.4	251.5	391.5	225.7	206.6	920.7	287.7	597	663.5
2	C=C	-35.36	0	38.81	74.15	524.1	787.6	270.6	526.1	182.6	448.8	37.85	449.1	214.5	240.9	163.9	61.11	749.3	0	336.9	318.9
3	ACH	-11.12	3.446	0	167	636.1	637.3	903.8	1329	25.77	347.3	5.994	-92.55	32.14	161.7	122.8	90.49	648.2	-4.449	212.5	537.4
4	ACCH ₂	-69.7	-113.6	-146.8	0	803.2	603.2	5695	884.9	-52.1	586.6	5688	115.2	213.1	0	-49.29	23.5	664.2	52.8	6096	603.8
5	OH	156.4	457	89.6	25.82	0	-137.1	353.5	-259.7	84	441.8	101.1	193.1	28.06	83.02	42.7	-323	-52.39	170	6.712	199
6	CH ₃ OH	16.51	-12.52	-50	-44.5	249.1	0	-181	-101.7	23.39	306.4	-10.72	193.4	-128.6	359.3	266	53.9	489.7	580.5	36.23	-289.5
7	H ₂ O	300	496.1	362.3	377.6	-229.1	289.6	0	324.5	-195.4	-257.3	72.87	0	540.5	48.89	168	304	-52.29	459	112.6	-14.09
8	ACOH	275.8	217.5	25.34	244.2	-451.6	-265.2	-601.8	0	-356.1	0	-449.4	0	0	0	0	0	119.9	-305.5	0	0
9	CH ₂ CO	26.76	42.92	140.1	365.8	164.5	108.7	472.5	-133.1	0	-37.36	-213.7	-38.47	-103.6	0	0	-169	6201	165.1	481.7	669.4
10	CHO	505.7	56.3	23.39	106	-404.8	-340.2	232.7	0	128	0	-110.3	11.31	304.1	0	0	0	0	0	0	0
11	CCOO	114.8	132.1	85.84	-170	245.4	249.6	200.8	-36.72	372.2	185.1	0	372.9	-235.7	0	-73.5	0	475.5	0	494.6	660.2
12	HCOO	90.49	-62.55	1967	2347	191.2	155.7	0	0	70.42	35.35	-261.1	0	0	0	0	0	0	0	0	-356.3
13	CH ₂ O	83.36	26.51	52.13	65.69	237.7	238.4	-314.7	0	191.1	-7.838	461.3	0	0	0	141.7	0	0	0	-18.51	664.6
14	CNH ₂	-30.48	1.163	-44.85	0	-164	-481.7	-330.4	0	0	0	0	0	0	0	63.72	-41.11	-200.7	0	0	0
15	CNH ₂	65.33	-28.7	-22.31	223	-150	-500.4	-448.2	0	0	0	136	0	-49.3	108.8	0	-189.2	0	0	0	0
16	(C) ₃ N	-83.98	-25.38	-223.9	109.9	28.6	-406.8	-598.8	0	225.3	0	0	0	0	38.89	865.9	0	0	0	0	0
17	ACNH ₂	1139	2000	247.5	762.8	-17.4	-118.1	-367.8	-253.1	-450.3	0	-294.8	0	0	-15.07	0	0	0	0	-281.6	0
18	PYRIDINE	-101.6	0	31.87	49.8	-132.3	-378.2	-332.9	-341.6	-51.54	0	0	0	0	0	0	0	0	0	-169.7	-153.7
19	CCN	24.82	-40.62	-22.97	-138.4	-185.4	157.8	242.8	0	-287.5	0	-266.6	0	38.81	0	0	0	777.4	134.3	0	0
20	COOH	315.3	1264	62.32	268.2	-151	1020	-66.17	0	-297.8	0	-256.3	312.5	-338.5	0	0	0	0	-313.5	0	0

† Adapted from xLUNIFAC Version 1.0

Subgroup Classification for TAEE Synthesis System

To calculation activity coefficient of each component in synthesis of TAEE from liquid phase of TAA and EtOH, the subgroups of the relevant species are as follows.



The parameters used in the UNIFAC calculation for this system are summarized in Table C.3 and Table C.4.

Table C.3 UNIFAC-VLE subgroup parameters (for TAEE system)[†]

Group	Main Group	Subgroup (k)	R _k	Q _k
CH3	1	1	0.9011	0.848
CH2	1	2	0.6744	0.540
C	1	4	0.2195	0.000
CH2=C	2	7	1.1173	0.988
CH=C	2	8	0.8886	0.676
OH	5	15	1.0000	1.200
H2O	7	17	0.9200	1.400
OCH2	13	26	0.9183	0.78

Table C.4 UNIFAC-VLE interaction parameters, a_{mk} , in Kelvins (for TAEE synthesis system)[†]

Group	Main Group	a_{mk}							
		CH3	CH2	C	CH2=C	CH=C	OH	H2O	OCH2
		1	1	1	2	2	5	7	13
CH3	1	0	0	0	86.02	86.02	986.5	1318	251.5
CH2	1	0	0	0	86.02	86.02	986.5	1318	251.5
C	1	0	0	0	86.02	86.02	986.5	1318	251.5
CH2=C	2	-35.36	-35.36	-35.36	0	0	524.1	270.6	214.5
CH=C	2	-35.36	-35.36	-35.36	0	0	524.1	270.6	214.5
OH	5	156.4	156.4	156.4	457	457	0	353.5	28.06
H2O	7	300	300	300	496.1	496.1	-229.1	0	540.5
OCH2	13	83.36	83.36	83.36	26.51	26.51	237.7	-314.7	0

[†] Adapted from xLUNIFAC Version 1.0

APPENDIX D

MODIFIED KINETIC PARAMETERS OF TAAE SYNTHESIS FOR APPLICATION IN ASPEN PLUS PROGRAM

Since it is not allowed to use the activity-based parameters in the ASPEN PLUS simulator, the kinetic parameters of PL model based on activity, shown in Table D.1, are converted to mole fraction forms by multiplying with average activity coefficient estimated from UNIFAC method (see Appendix C for details). Table D.2 shows the average activity coefficients that are calculated by using MATLAB. The modified kinetic parameters are obtained by calculating the rate parameters at several temperature levels (333 343 and 353 K).

Table D.1. The values of kinetic constant and activation energy in activity-based PL model

Kinetic Parameter of PL.A model	Activation Energy, <i>E_a</i> (kJ/mole)
$k_{1,a} = \exp(35.8-14050/T)$	116.8
$k_{-1,a} = \exp(35.1-14146.2/T)$	117.6
$k_{2,a} = \exp(20.77-8840.3/T)$	73.5
$k_{-2,a} = \exp(10.7-5652/T)$	47.0
$k_{3,a} = \exp(33-14900/T)$	123.9
$k_{-3,a} = \exp(42.358-18183.6/T)$	151.2
$K_{eq1,a} = \exp(0.702+96.2/T)$	
$K_{eq2,a} = \exp(10.06-3187.4/T)$	
$K_{eq3,a} = \exp(-9.358+3283.6/T)$	

Table D.2. Average activity coefficient calculated by MATLAB

Temperature (K)	Activity coefficient (average)				
	H2O	EtOH	TAA	TAAE	IA
333	3.01	1.06	1.02	1.94	3.16
343	2.99	1.07	1.02	1.79	3.06
353	3.03	1.08	1.02	1.81	2.99

The input rate expressions for Aspen Plus are in the following equations:

$$r_{1,x} = r_{\text{Etherification of TAA}} = k_{1,x}x_{\text{TAA}}x_{\text{EtOH}} + k_{-1,x}x_{\text{TAAE}}x_{\text{H}_2\text{O}} \quad (\text{D-1})$$

$$r_{2,x} = r_{\text{Dehydration}} = k_{2,x}x_{\text{TAA}} + k_{-2,x}x_{\text{H}_2\text{O}}x_{\text{IA}} \quad (\text{D-2})$$

$$r_{3,x} = r_{\text{Etherification of IA}} = k_{3,x}x_{\text{IA}}x_{\text{EtOH}} + k_{-3,x}x_{\text{TAAE}} \quad (\text{D-3})$$

The following example shows how to convert the kinetic parameters based on activity form to those based on mole fraction form. For the reaction rate of EtOH in activity form, as given in Eq. (D-4),

$$r_{1,a} = r_{\text{Etherification of TAA}} = k_{1,a}a_{\text{TAA}}a_{\text{EtOH}} + k_{-1,a}a_{\text{TAAE}}a_{\text{H}_2\text{O}} \quad (\text{D-4})$$

The relationship of activity and mole fraction is given in the Eq. (D-5)

$$a_i = \gamma_i x_i \quad (\text{D-5})$$

Substituting the activity of each component (a_i), shown in Eq. (D-5), in Eq. (D-4), the following expression is obtained

$$r_{1,a} = r_{\text{Etherification of TAA}} = k_{1,a} * (\gamma_{\text{EtOH}} \gamma_{\text{TAA}}) x_{\text{TAA}} x_{\text{EtOH}} + k_{-1,a} * (\gamma_{\text{TAAE}} \gamma_{\text{H}_2\text{O}}) x_{\text{TAAE}} x_{\text{H}_2\text{O}} \quad (\text{D-6})$$

and rearranging the kinetic parameters, we obtain

$$k_{1,x} = k_{1,a} * (\gamma_{\text{EtOH}} \gamma_{\text{TAA}}) \quad (\text{D-7})$$

$$k_{-1,x} = k_{-1,a} * (\gamma_{TAAE} \gamma_{H_2O}) \quad (D-8)$$

Next, the new value of the modified kinetic parameters based on average activity coefficients (Table D.2) is calculated at several temperature levels as follows.

$$\begin{aligned} \text{At } T = 333\text{K}, \quad k_{1,x} &= k_{1,a} * (\gamma_{EtOH} \gamma_{TAA}) \\ k_{1,x} &= \exp(35.8 - 14050/333) * (1.06 * 1.02) \\ k_{1,x} &= 0.0045 \end{aligned}$$

With the same method of calculation as shown above, the new value of the kinetic parameter, $k_1(new)$, at various temperature is obtained:

$$\begin{aligned} \text{At } T = 333 \quad k_{1,x} &= 0.0018 \\ \text{At } T = 343 \quad k_{1,x} &= 0.0063 \\ \text{At } T = 353 \quad k_{1,x} &= 0.02 \end{aligned}$$

Then, the Arrhenius plot ($\ln k_1$ versus $1/T$) as shown in Figure D.1 is made to find the new rate expression of the kinetic constant, $k_1(new)$.

From Figure D.1, we obtain the rate expression of $k_1(new)$ as follows,

$$k_{1,x} = \exp(36.154 - 14142/T)$$

and the activation energy is

$$E_a = 14142 * 8.314 / 1000 = 11756.6 \quad (\text{J/mole})$$

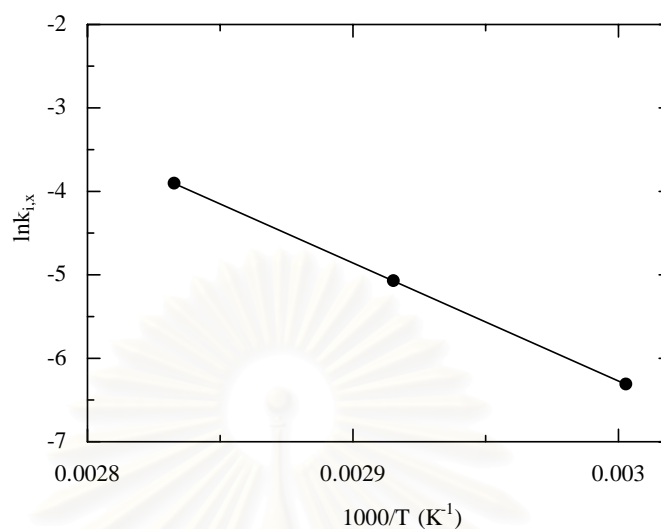


Figure D.1 Arrhenius's plot of $k_{1,x}$ in ln scale

Table D.3 summarizes other modified kinetic parameters which are based on rate expression in mole fraction form and used in ASPEN Plus.

Table D.3. Modified kinetic constant and activation energy for this study

Kinetic Parameter based on mole fraction (mole/s*meq H ⁺)	Activation Energy, E_a (kJ/mole)
$k_{1,x} = \exp(36.154 - 14142/T)$	117.6
$k_{-1,x} = \exp(35.601 - 13731/T)$	114.2
$K_{2,x} = \exp(20.746 - 8825.7/T)$	73.4
$k_{-2,x} = \exp(12.079 - 5359.5/T)$	44.6
$k_{3,x} = \exp(33.577 - 14690/T)$	122.1
$k_{-3,x} = \exp(41.691 - 17745/T)$	147.5
$K_{eq1,x} = \exp(0.553 - 411.2/T)$	
$K_{eq2,x} = \exp(8.667 - 3466.2/T)$	
$K_{eq3,x} = \exp(-8.114 + 3055/T)$	

VITA

Miss Onkanok Boonthamtirawuti was born on September 11, 1981 in Bangkok, Thailand. She obtained the bachelor's degree in industrial chemical science from King Mongkut's Institute of Technology Ladkrabang (KMIT'L), Bangkok, in May, 2003. Then she continued her Master degree in Chemical Engineering at Chulalongkorn University and graduated in June, 2006.



สถาบันวิทยบริการ
จุฬาลงกรณ์มหาวิทยาลัย